

Predicting degraded lifting capacity of aging tower cranes: A digital twin-driven approach

Mudasir Hussain^a, Zhongnan Ye^a, Hung-Lin Chi^{b*}, Shu-Chien Hsu^a

^a Department of Civil and Environmental Engineering, The Hong Kong Polytechnic University, Hong Kong

^b Department of Building and Real-Estate, The Hong Kong Polytechnic University, Hong Kong

mudasir.hussain@connect.polyu.hk, zhong-nan.ye@connect.polyu.hk, hung-lin.chi@polyu.edu.hk,
mark.hsu@polyu.edu.hk

Corresponding Author: Hung-Lin Chi; Email: hung-lin.chi@polyu.edu.hk; ORCID ID: 0000-0003-0756-4864

Highlights

- A digital twin-driven (DTD) framework and model are developed for predicting degraded lifting capacity (LC) of aging tower cranes.
- A DTD model predicted the degraded LC of a scaled-down prototype, achieving a mean-square error (MSE) of 0.2253 and a coefficient of determination (R^2) of 0.9973.
- A DTD model is validated using k-5 cross-validation with a prediction accuracy of 0.97 (R^2).
- Degraded load charts assist operators in placing safe loads and preventing unexpected failures.

Abstract

Aging tower cranes face an elevated risk of failure, primarily due to structural fatigue and deterioration. Surprisingly, the degradation of aging-induced lifting capacity (LC) remains an unexplored domain. In response to this research gap, this paper introduces a digital twin-driven (DTD) framework and model to predict the degraded LC of aging tower cranes. This framework combines theoretical and numerical analysis of fatigue and degradation behavior in tower cranes with real-time vibration data obtained during cyclic load scenarios on the actual cranes. Machine learning (ML) techniques are employed to develop a model that accurately predicts the degraded LC caused by aging. A scaled-down tower crane prototype is adopted as a demonstrative case to illustrate the feasibility and effectiveness of the DTD framework. The DTD model predicts the degraded LC of the prototype with high accuracy, achieving a mean-square error (MSE) of 0.2253 and a coefficient of determination (R^2) of 0.9973. The predicted degraded load charts of the tested tower crane for each decade of usage from 0 to 70 years are also presented to assist crane operators in applying safe loads, preventing unexpected failures and damages, and enhancing workplace monitoring and safety. This study helps monitor the safety conditions of tower cranes that are aging and susceptible to structural fatigue and deterioration, facilitates the prediction of the deterioration of complex machines and systems in the construction industry with real-time data, and highlights the potential of DTD approaches in improving efficiency, safety, and decision-making.

Keywords: Tower crane, Digital twin, Lifting capacity, Safety monitoring, IoT system

39 1. Introduction

40 Tower cranes are essential in modern construction projects, facilitating the lifting and
41 moving of hefty modules, equipment, and tools from lifting points to target locations on
42 construction sites [1]. Over prolonged periods of use, however, aging tower cranes may
43 experience structural fatigue, corrosion, and deterioration due to exposure to high-cycle and
44 variable-amplitude loads, harsh working environments, and improper operation and
45 maintenance, leading to degraded lifting capacity (LC) [2–8]. Such degradation can increase
46 the risk of accidents and jeopardize the safety of workers and nearby properties, resulting in
47 severe injuries or fatalities [9]. For instance, in 2022, the tower crane at the "Sau Mau Ping"
48 construction site in Hong Kong collapsed and killed three workers, where the operator set the
49 manufacturer-specified load without considering the deteriorated load and/or capacity [10].
50 Similar incidents have occurred worldwide, including a crane collapse that killed 18 people in
51 2016 in Dongguan, China [11], and another crane collapse that killed seven people and injured
52 dozens more in 2008 in New York City in the United States [12]. Thus, there is still a practical
53 need for real-time safety monitoring systems to detect and prevent accidents caused by aging
54 tower cranes with degraded LC.

55 Various safety monitoring systems have been developed and adopted in the construction
56 industry to address crane safety, including load moment indicators (LMIs) [13–16], anti-two-
57 blocking (ATB) systems [17, 18], and crane cameras [19, 20]. LMIs measure the load on the
58 crane and provide a warning when the load is near or exceeds the crane's maximum LC [13].
59 Anti-two-block systems prevent the crane from collapsing by limiting its operation when the
60 hook block is too close to the boom tip [18]. Crane cameras monitor the crane's movement and
61 detect unsafe behavior by recording a visual perspective [20]. However, while these systems
62 can improve safety on construction sites, they are generally not designed to address the specific
63 issue of aging tower cranes with degraded LC. For instance, LMIs, ATB systems, and crane
64 cameras do not consider the effects of wear and tear on crane components or the health level
65 of the crane and, thus, fail to predict the internal degradation in LC, which can result in
66 unexpected accidents due to unintentional over-loading. Furthermore, due to the unavailability
67 of historical data on crane operations, the complexity of the deterioration mechanism itself, and
68 the unpredictability of external deterioration-related factors, it remains an open question of how
69 to estimate and update the aging-induced LC degradation.

70 Many studies have been conducted to tackle the issues of data availability and deterioration
71 mechanism in understanding the degraded LC of tower cranes, which can be categorized into
72 two groups: (1) data-driven methods (DDM) and (2) model-based methods (MBM). DDM uses
73 real-time, historical, and maintenance data [21] to predict deterioration patterns [22]. Several
74 studies have used DDM to predict performance degradation in tower cranes [23]. However,
75 DDM is only effective when data are abundant, and without proper domain knowledge of the
76 deterioration mechanisms, it may be less reliable when applied practically. On the other hand,
77 MBM requires an understanding of failure mechanisms such as cracks, wear, deflection,
78 friction, and stress. One can estimate performance degradation by developing a mathematical
79 model that quantitatively describes the crane's degradation. However, extensive experiments
80 are required for parameter identification, varying from case to case. Due to the complex nature

81 of tower cranes, MBM may be less efficient. To overcome the limitations of DDM and MBM,
82 Liu et al. [24] proposed a hybrid approach that combines both methods (DDM-MBM). This
83 approach collects data from multiple sensors since a single sensor cannot capture all the
84 relevant parameters that affect degradation. The use of multiple sensors may increase
85 complexity, but it results in more accurate predictions. Additionally, the mechanical model
86 used in MBM can simulate the structural performance of the tower crane, which increases the
87 interpretability of DDM. Therefore, a hybrid approach that integrates multi-sensor data with
88 an interpretable model could be a possible solution to enable real-time monitoring and
89 prediction of tower cranes' safety conditions considering degraded LC.

90 As an instance of hybrid DDM-MBM methods, the digital twin-driven (DTD) approach
91 creates a replica of a physical system, aiming to enable real-time data acquisition, response
92 prediction, and human-machine interaction (HMI) [25]. The DTD approach has been widely
93 utilized across various studies for various applications, including product design,
94 manufacturing, planning, maintenance, management, control, traceability, anomaly detection,
95 operational errors, and safety analysis [26–36]. For instance, in a study by Yang et al. [37], a
96 hybrid DTD approach was used to predict the performance degradation in the transmission unit
97 of CNC machines by incorporating damage indices with wear data from Achard wear theory.
98 Similarly, Tran et al. [23] predicted machine degradation by considering both the present
99 conditions of the machine and degradation indices based on a year of data. However, these
100 methods are time-consuming and primarily applicable only to those tools. Despite the extensive
101 use of DT in the degradation field, there is limited research exploring the potential of the DTD
102 approach in predicting the deterioration of complex machines and systems in the construction
103 industry using real-time data. Nevertheless, the mentioned examples from adjacent fields
104 highlight the flexibility and potential of the DTD approach in improving efficiency, safety, and
105 decision-making in various applications.

106 Aiming to address the real-time safety monitoring and alerting of aging tower cranes, this
107 study develops a DTD framework and model to predict degraded LC after different usage
108 periods. The framework integrates theoretical and numerical analyses of tower crane fatigue
109 and degradation behavior with real-time vibration data obtained during cyclic load scenarios
110 on the physical tower crane. Machine learning (ML) models, including Random Forest (RF)
111 and Support Vector Machine (SVM), are employed for feature selection and LC prediction.
112 Specifically, a scaled-down tower crane prototype is adopted as a demonstrative case to
113 illustrate the feasibility and effectiveness of the DTD framework. The predicted degraded load
114 charts of the prototype for each decade of usage from 0 to 70 years are presented for validation
115 purposes. The proposed DTD framework allows for continuous monitoring of the crane's safety
116 performance considering the degradation in LC with real-time data and numerical model,
117 which is expected to significantly improve safety in construction sites with aging tower cranes.

118 This paper is structured as follows: [Section 2](#) presents a comprehensive review of the
119 existing research and studies related to the topic; [Section 3](#) presents a DTD framework for
120 monitoring machine deterioration, explicitly focusing on the theoretical background of DTD
121 approaches and numerical analysis of tower crane fatigue accumulation and degradation in LC;
122 and [Section 4](#) outlines the process of developing a DTD model for tower crane degradation

123 prediction. In [Section 5](#), a case study is conducted using a physical prototype of a tower crane
124 to evaluate the accuracy, efficiency, and applicability of the DTD model. [Section 6](#) discusses
125 the findings of the study. Finally, [Section 7](#) provides concluding remarks, limitations, and
126 directions for future research.

127 **2. Literature review**

128 **2.1. Crane safety in construction projects**

129 Construction sites are widely recognized as challenging environments due to the
130 simultaneous and complex nature of multiple hazardous activities. These activities involve the
131 movement of laborers, heavy machinery, and construction materials, thereby amplifying the
132 associated risks [38]. Cranes, being a crucial piece of equipment in construction, not only play
133 a significant role but also pose substantial health and safety concerns for their operators.

134 Previous research has focused on understanding the causes of injuries and fatalities related
135 to various crane activities, including layout planning, installation/dismantling, erection, and
136 operations. These studies aimed to identify the key factors contributing to crane accidents. For
137 instance, Sulankivi et al. [39] investigated safety issues in crane layout planning, whereas Shin
138 [40] identified the primary factors influencing crane safety during installation and dismantling
139 processes. Chang et al. [41] used 3D simulation and visualization techniques to improve safety
140 during crane erection. Sadeghi et al. [42] developed a framework for ensemble risk analysis to
141 enhance the safety of crane operations. Shapira et al. [43] identified 20 factors associated with
142 crane safety, including project conditions, environmental factors, human factors, and safety
143 management. Finally, Lee et al. [9] found that most crane accidents occur because of human
144 error and crane-related issues. Crane-related problems include structural fatigue, wear and tear,
145 stress, strain, cracks, corrosion, deterioration, and the risk of structural collapse. These issues
146 arise from exposure to cyclic and varying loads, challenging working conditions, and
147 inadequate operation and maintenance practices. As a result, the LC of the cranes decreased
148 over time. Research studies are essential to identify and quantify the degradation of LC caused
149 by the aging of these cranes.

150 **2.2. Analytical approach for crane degradation**

151 Analytical methods use tools, models, mathematical equations, and formulas to address
152 complex problems. In crane assessment, these techniques are applied to evaluate and predict
153 factors such as structural integrity, LC, and overall safety. This approach involves
154 understanding failure mechanisms such as cracks, wear and tear, deflection, friction, and stress,
155 identifying critical components, considering environmental conditions, and analyzing
156 historical data. Relevant information regarding crane usage, environmental factors, and
157 material properties is collected and organized for analysis. Monitoring indicators of early
158 degradation throughout the crane's operational lifespan can help detect potential issues in
159 advance.

160 Researchers have studied various critical components of the crane to investigate specific
161 failure mechanisms. For instance, Vukelic et al. [44] investigated the failure mechanism of
162 crane gear damage, while Guerra-Fuentes et al. [45] studied the failure analysis of steel wire
163 ropes in overhead crane systems. Das et al. [7] reviewed the failure analysis of hooks, and Wu

164 et al. [46] developed models for fatigue damage accumulation in critical components exposed
165 to moving loads. Experimental and numerical methods are employed to examine component
166 behavior and identify the root causes of failure. Experimental techniques involve visual
167 inspections, chemical composition analysis, mechanical properties, and hardness tests.
168 Numerical methods, such as finite element analysis (FEA), are utilized to calculate stress/strain
169 and load/deflection, providing insights into the structural performance of crane components.
170 However, it is essential to acknowledge that the analytical method has limitations. It requires
171 a comprehensive understanding of each parameter used in the model and extensive
172 experimental work to comprehend the failure mechanisms of individual components.
173 Therefore, this method may be less effective for complex machines like cranes, as it relies on
174 assumptions and suppositions regarding various parameters.

175 **2.3. Data-driven method for crane degradation**

176 A data-driven method (DDM) analyzes and interprets data to address problems and make
177 informed decisions. It utilizes statistical, machine learning (ML), or artificial intelligence (AI)
178 techniques to collect and scrutinize relevant data related to the degradation of tower cranes.
179 The main goals of this approach are to monitor the operational state and performance of the
180 cranes, predict potential issues or failures, and optimize maintenance and operational strategies.
181 Various types of data are considered, including operational data (e.g., load, usage, and
182 environmental conditions), sensor data (e.g., vibration and temperature), maintenance records,
183 and historical failure data. A thorough analysis of this data is conducted to identify patterns
184 and trends.

185 For example, Tran et al. [23] conducted a study where they employed a support vector
186 machine (SVM) to predict machine degradation and estimate the remaining useful life (RUL)
187 of machines. They incorporated monitoring and operational data, along with degradation
188 indices, to establish a failure threshold for decision-making. However, it is important to note
189 that the effectiveness of the DDM approach relies on having sufficient data available, and
190 without a solid understanding of the specific domain's deterioration mechanisms, its practical
191 application may be less reliable. Additionally, the data in this particular study was sourced
192 from only one or two sensors installed over the course of a year.

193 To overcome this issue, Roman et al. [22] introduced a hybrid data-driven fuzzy active
194 disturbance rejection control system for tower cranes. Similarly, Liu et al. [24] utilized hybrid
195 deep neural networks to assess machine performance based on fatigue data. The hybrid
196 approach involves collecting data from multiple sensors, but it can result in complex and
197 computationally intensive modeling due to the increased data volume. This is where the digital
198 twin-driven (DTD) method comes into play, as it allows for real-time data acquisition,
199 prediction of responses, and interaction between humans and machines.

200 **2.4. Digital twin-driven method for crane degradation**

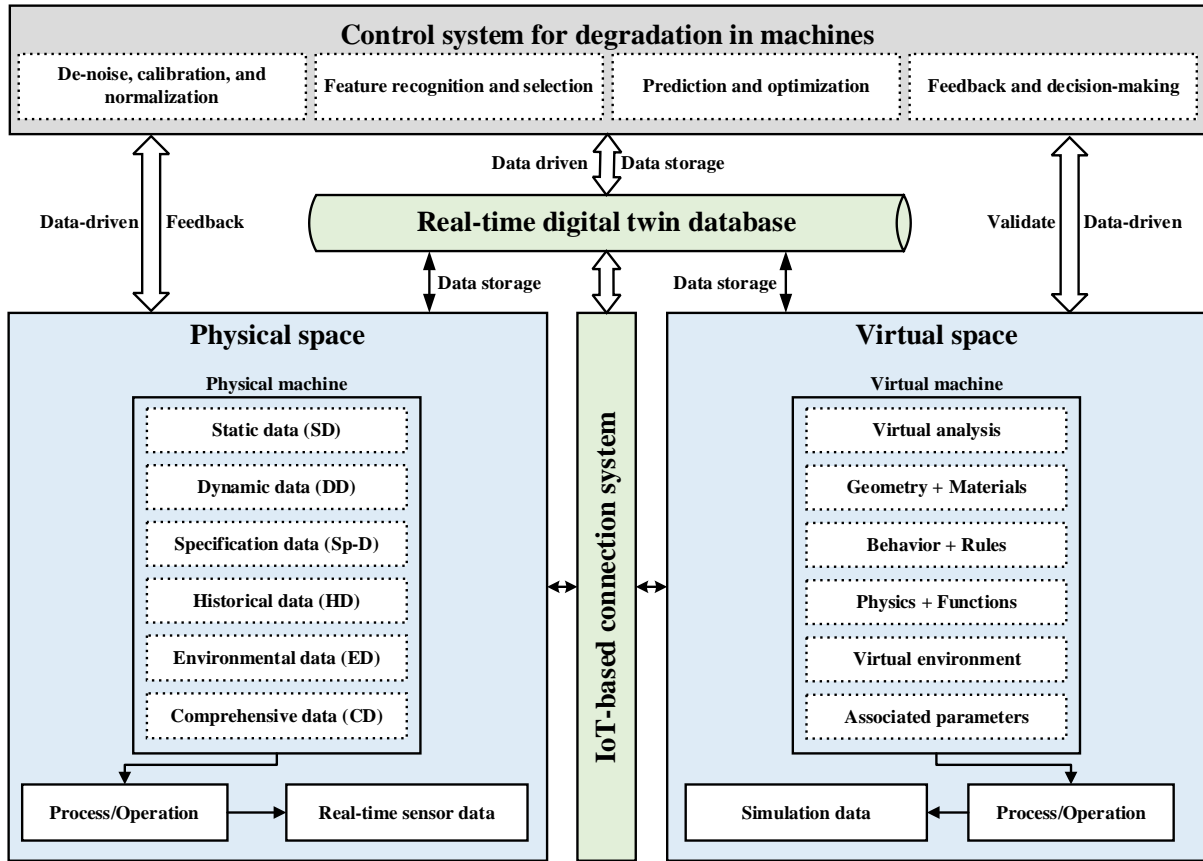
201 A digital twin-driven (DTD) approach utilizes digital twin technology to monitor the
202 operational condition, performance, and potential degradation of a complex physical system,
203 such as tower cranes. A digital twin is a virtual replica of the physical object created through
204 advanced data analytics, simulation, and modeling techniques. Researchers have applied DTD

205 technology to address various machine performance degradation problems. For instance,
206 Deebak et al. [26] used the DTD method for fault diagnosis in machining tool conditions. In
207 contrast, Zhu et al. [32] used it to control the machining process for thin-walled part
208 manufacturing. Zhang et al. [47] utilized DTD for surface roughness prediction, and Liu et al.
209 [29] employed it for traceability and dynamic control of machine processes. Zhuang et al. [48]
210 utilized DTD to predict wear in the turning process of machines. Jiang et al. [25] focused on
211 the stability analysis of the tower crane hoisting process by examining stress conditions during
212 various hoisting scenarios. Finally, Yang et al. [37] used DTD for performance degradation in
213 the transmission unit of CNC machine tools. However, their approach involved incorporating
214 damage indices with wear data from a specific model, making it time-consuming, complex,
215 and applicable only to that particular tool. Therefore, this study proposes a method for
216 predicting degradation in aging tower cranes based on real-time data, offering a more efficient
217 and versatile approach.

218 **3. Methodology**

219 **3.1. A digital twin-driven framework for degradation in machines**

220 The primary goal of this study is to use a DTD approach to predict degradation in machines,
221 such as tower cranes. A DTD framework is formulated based on the mapping between physical
222 and virtual machines, as illustrated in Fig. 1. This framework aims to (1) provide background
223 information, (2) highlight issues, (3) define data requirements, (4) simplify mapping problems
224 between virtual-physical spaces, (5) establish two-way communications between all parts, and
225 (6) make decisions and feedback for improvement. A DTD approach for degradation must have
226 five parts: physical space, virtual space, IoT-based connection, real-time database, and control
227 system [49–51]. Machine degradation is predicted by mapping or fusing the DTD components
228 using DT data.



229

230 **Fig. 1.** A digital twin-driven framework for predicting degradation in machines.

231 **3.1.1. Physical space**

232 The physical space module encompasses all the physical activities, operational processes,
 233 and work environments contributing to degradation monitoring [25]. To enhance the accuracy
 234 and effectiveness of the DTD model, it is crucial to collect data related to element
 235 compositions, dynamics, failure mechanisms, and deterioration factors [31]. This requires the
 236 installation of sensors and transducers with networking capabilities (such as Wi-Fi or Ethernet)
 237 on the physical machine to collect real-time, multi-source, and heterogeneous data. The
 238 physical machine may also have a built-in data logging system that records usage information
 239 [52]. [Section 4.1](#) will provide a detailed explanation of the various types of additional data
 240 required to improve the quality of the DTD model, including static data (SD), specification
 241 data (Sp-D), historical data (HD), environmental data (ED), and comprehensive data (CD).
 242 Once the necessary data from both the physical and virtual space is collected and a two-way
 243 connection is established, decisions can be made, and feedback can be provided for machine
 244 monitoring, control, safety, and improvement. The physical space module represents the
 245 environment in which the tower crane operates, encompassing the crane structure, components,
 246 and relevant sensors for data collection. The significance of this module is highlighted in its
 247 role in capturing real-time operational data and physical conditions.

248 **3.1.2. Virtual space**

249 For a DTD approach, it is essential to have a CAD model or virtual representation that
 250 accurately captures the machine's features, geometry, materials, behaviors, physics, rules,

251 functions, and environment [53, 54]. The level of detail (LOD) of the virtual model may vary
252 depending on the specific case and desired data fidelity [47, 55]. With high data fidelity from
253 the physical space, the static virtual body comes to life, reflecting the element composition,
254 dynamics, and real-time status of the physical machine in the virtual environment. Its primary
255 purpose is to provide a realistic description and dynamic simulation of physical entities and
256 processes across multiple dimensions and time scales [25]. The virtual body offers an open
257 interface for data-driven modeling (DDM), optimization, and the ability to predict the current
258 status and remaining useful life (RUL) of the physical machine [52]. In this module, digital
259 twin technology is employed to create a virtual replica of the tower crane. The significance of
260 this module has been clarified, emphasizing its role as a digital representation of the physical
261 crane. This representation allows for the simulation and analysis of the crane's behavior under
262 various operating conditions.

263 **3.1.3. IoT-based connection**

264 In accordance with ISO/OSI communication standards, the communication system for the
265 DTD model can be implemented using either wired or wireless technologies [56]. To establish
266 real-time data transfer and parsing, an IoT-based connection is utilized. This connection serves
267 as a crucial link that facilitates two-way communication between physical and virtual spaces.
268 It ensures that all components of the DTD model are integrated and appropriately mapped to
269 detect and respond to real-time changes in the physical space, as well as to receive feedback
270 from the control system [28, 57]. Additionally, this module ensures secure connection and data
271 transmission between the physical machine and the virtual machine in both directions. Its
272 significance lies in establishing connectivity between the physical and virtual spaces, thereby
273 enabling seamless data flow and real-time synchronization between the physical tower crane
274 and its digital twin.

275 **3.1.4. Real-time digital twin database**

276 Real-time data from the digital twin is utilized to integrate the multi-dimensional and multi-
277 scale virtual simulation model with the physical model and control system. Data serves as the
278 foundational concept of the DTD model, enabling the virtual model to execute operations and
279 make informed decisions. This module is crucial in interpreting, classifying, storing, pre-
280 processing, maintaining, and testing data [26]. This module is responsible for storing and
281 managing the data collected from both the physical crane and its digital twin. The module's
282 significance has been detailed, highlighting its role in storing historical data, enabling
283 comparison and analysis, and supporting predictive maintenance decision-making. The DTD
284 model can effectively access and utilize the collected data for various tasks and processes by
285 leveraging this module.

286 **3.1.5. Control system**

287 The control system within the DTD model plays a vital role in regulating and predicting
288 degradation based on real-time data from the digital twin. It represents the hybrid mode and
289 serves as the most fundamental phase of the DTD model. The control system is responsible for
290 analyzing, visualizing, making decisions, and providing feedback for improvement [47]. It
291 consists of two main components: (1) data pre-processing and (2) a functional module. The

292 data pre-processing component is primarily responsible for tasks such as online monitoring,
293 de-noising, calibration, normalization, analysis, statistics, and evaluation of raw and real-time
294 data collected from both physical and virtual spaces [31]. This module also includes feature
295 recognition and selection, which is crucial in identifying degradation factors [58]. The
296 functional module incorporates both prediction and visual display capabilities [52]. The
297 predicted results are utilized for decision-making and improvement of the physical machine
298 through feedback. Operators or decision-making teams can directly implement optimization
299 and adjustment plans based on the insights provided. The control system module forms the core
300 of the DTD framework. The crucial role of this module has been clarified by explaining that it
301 integrates data from the physical and virtual spaces, performs real-time monitoring and
302 analysis, and enables decision-making and feedback loops for proactive maintenance and
303 performance optimization.

304 **3.2. Fatigue behavior and deterioration in cranes**

305 Tower cranes are considered to be structures prone to fatigue and are at risk of collapsing
306 during operation [24, 59]. In terms of fatigue behavior, tower cranes are classified as high-
307 cycle and super-high-cycle fatigue structures based on the S-N curve, also known as the fatigue
308 curve or Wohler curve [60]. The fatigue curve represents the relationship between the cyclic
309 stress amplitude and the number of cycles until failure. To analyze fatigue behavior in tower
310 cranes, various approaches can be employed, including stress-life, strain-life, non-destructive,
311 fracture mechanics, and damage mechanics.

312 The stress-life approach involves plotting stress against the number of cycles until failure
313 [61]. However, this approach requires extensive experimental data, and a single stress-life plot
314 has limitations when it comes to predicting plasticity, deformation, and mean stress. Similarly,
315 the strain-life method entails plotting strain against the number of cycles until failure [62]. This
316 approach requires the stress-strain curve and consideration of plasticity nucleation to determine
317 the transition life between plastic and elastic regions under fatigue loading. Therefore, it is
318 mainly applicable when determining the crack initiation life of the crane structure. Non-
319 destructive techniques can be used to study fatigue by measuring and analyzing inherent
320 properties such as cracks, strength reduction, and stiffness degradation [63]. However, this
321 method necessitates a comprehensive understanding of the relevant parameters and can be
322 challenging to cover all aspects [24]. In fracture mechanics, the focus is on pre-existing flaws
323 and micro-cracks in the structure [64]. The degradation rate is determined using a crack growth
324 law and stress intensity factor as a function of crack depth, shape factor, and stress range.
325 However, our study doesn't consider crane sections with pre-existing defects. Finally, damage
326 mechanics use appropriate assessment models, laws, and patterns to characterize damages,
327 residual stresses, and strain localization [60, 64–66]. Damage mechanics is a suitable approach
328 for addressing tower crane degradation as it encompasses critical factors that directly and
329 indirectly influence crane degradation. For example, micro-plastic strain is often overlooked in
330 low-cycle fatigue problems, but it must be considered in the case of high-cycle or super-high-
331 cycle fatigue damage within the elastic range, as is the case with tower cranes. Macro-plastic
332 strain can result from such scenarios, leading to structural deterioration under long-term
333 operational loading.

334 While steel structures can have an infinite design life if the stress range is low, tower cranes
335 are prone to fatigue due to the cyclic and varied stress amplitudes experienced by their
336 components during operation. For instance, when a tower crane lifts a heavy load at full stretch
337 and lifting radius, it experiences a higher stress range. Additionally, the loads exerted on the
338 crane are cyclic and have varying amplitudes. As a result, elastic deformation occurs in the
339 crane structure, generating stress and accumulating residual stresses over time. When the
340 residual stresses reach a critical threshold, cracks form, posing a collapse risk for the crane.
341 Therefore, measuring the loads and the associated deflection, deformation, and vibration of the
342 physical tower crane is crucial to predicting degradation accurately.

343 **3.2.1. Fatigue damage accumulation analysis for cranes**

344 There are two main approaches for evaluating fatigue damage: (1) constant amplitude
345 fatigue loading and (2) variable amplitude fatigue loading. In the case of a tower crane, the
346 loads it experiences are stochastic and cyclic, causing fatigue damage accumulation to vary
347 with each loading cycle. As a result, the traditional linear cumulative damage criterion is not
348 applicable in the context of tower cranes [67]. Instead, non-linear and double-linear damage
349 rules are used to account for variable amplitude loads [68].

350 During the progression of variable amplitude fatigue loading, the tower crane structure
351 undergoes irreversible deformations and accumulates residual stresses. These factors
352 contribute to the initiation and propagation of cracks within the structure. The presence of
353 residual stresses causes cracks to propagate along a particular plane once initiated. These
354 irreversible local deformations and crack propagation significantly impact the overall stability
355 and reliability of the tower crane.

356 Various parameters can be employed to analyze the damage occurring in the tower crane
357 structure, including total strain, residual stress, stiffness degradation, strength degradation, heat
358 dissipation resulting from micro-cracking, crack propagation, and the speed of sound. In our
359 study, we simulate the mechanical response of the crane structure by considering stress,
360 displacement, and damage index while applying a moving load with variable amplitude.

361 Existing literature [24, 46, 60, 64–71] indicates that the damage rate in the tower crane is
362 influenced by multiple variables, as expressed in Eq. (1). These variables are used to determine
363 the damage rate of the tower crane structure.

$$364 \quad dD = f(\sigma_M, \bar{\sigma}, D, \Delta\sigma)dN \quad (1)$$

365 where dD is the damage rate, σ_M is the maximum stress, $\bar{\sigma}$ is the mean stress, D is the current
366 damage state, $\Delta\sigma$ is the stress spectrum in one cycle, and N is the number of cycles.

367 **3.2.2. Finite-element analysis for degradation index and degradation rate**

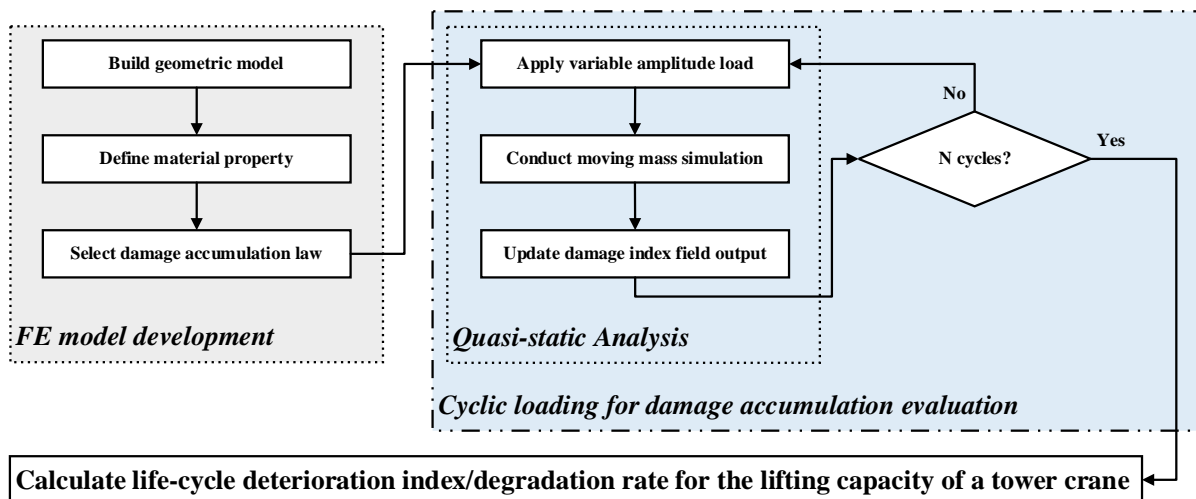
368 To assess the accumulation of fatigue damage in the crane structure over a 70-year
369 operational period, we follow the procedure outlined in Fig. 2. While the estimated life
370 expectancy of a tower crane is typically 50-60 years [46, 72], we have chosen to extend the
371 analysis to 70 years in order to enhance the quality and accuracy of the DTD model.

372 First, we developed a finite element model (FEM) that incorporates the geometric
 373 specifications and material properties of the tower crane. This FEM model allows us to analyze
 374 the structural performance of the crane under working conditions over a 70-year period.
 375 Subsequently, we apply moving loads with variable amplitude to the crane cyclically,
 376 considering the material's damage accumulation behavior. This approach allows us to simulate
 377 the mechanical response of the crane, including stress, displacement, and damage index.

378 Fig. 3 provides an example of the damage index contours for a simulated tower crane after
 379 10, 20, 30, 40, 50, 60, and 70 years of operations. A damage index value of zero indicates no
 380 damage to the crane, While one suggests complete fatigue-induced damage to the crane model.
 381 In this context, the degradation rate (dD) is determined by subtracting the damage index from
 382 one, as indicated in Eq. (2).

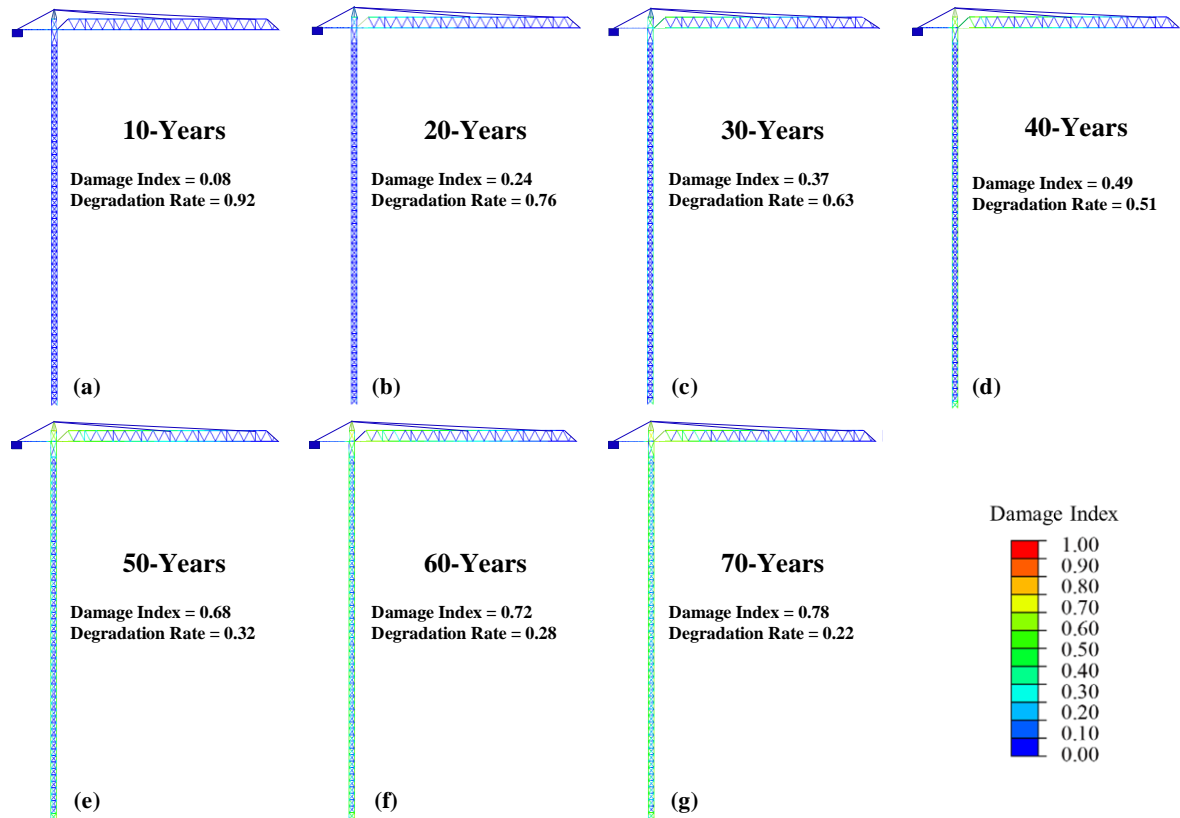
$$dD = 1 - dI \tag{2}$$

383 where dD denotes the damage rate, and dI denotes the damage index, which varies from 0 to
 384 1.



385

386 Fig. 2. Numerical procedure for a tower crane's fatigue damage accumulation modeling.



387

388 **Fig. 3.** Fatigue damage accumulation analysis: (a) 10-Years, (b) 20-Years, (c) 30-Years, (d)
 389 40-Years, (e) 50-Years, (f) 60-Years, and (g) 70-Years.

390 3.3. Data incorporation for degradation

391 In previous studies, Yang et al. [37] and Tran et al. [23] employed a hybrid model (DDM
 392 and MBM) that fused damage indices with real-time sensory data to predict machinery
 393 performance degradation. In our proposed DTD model, cumulative residual stress values are
 394 integrated as “damage indices” to assess the degradation of tower cranes under cyclic loads
 395 over operational periods of 10 to 70 years. These damage indices were derived from virtual
 396 simulations of tower crane behavior and seamlessly merged with real-time sensory data,
 397 including crane vibrations and load information. The combined dataset is securely stored in a
 398 real-time database, such as Firebase, facilitating continuous analysis and monitoring in real-
 399 time; stepwise details are included in [Section 4](#).

400 Following data storage, the DTD model incorporates a pre-processing module that conducts
 401 temporal analysis of the sensory data, encompassing time- and frequency-domain techniques
 402 to extract relevant features capturing load-induced degradation in tower cranes. These features
 403 precisely depict the relationships between load, deflection, and fatigue damage resulting from
 404 cyclic loading. As the damage indices cover various aspects of the applied loads and their
 405 corresponding deflections, ongoing data analysis uses stress-strain or load-deflection methods,
 406 as outlined in [Section 5](#). This involves a comparison of the stress concentrations resulting from
 407 the loading cycles to those associated with structural failure. This evaluation allowed the DTD
 408 model to train and test a machine learning (ML) model using labeled data. It establishes

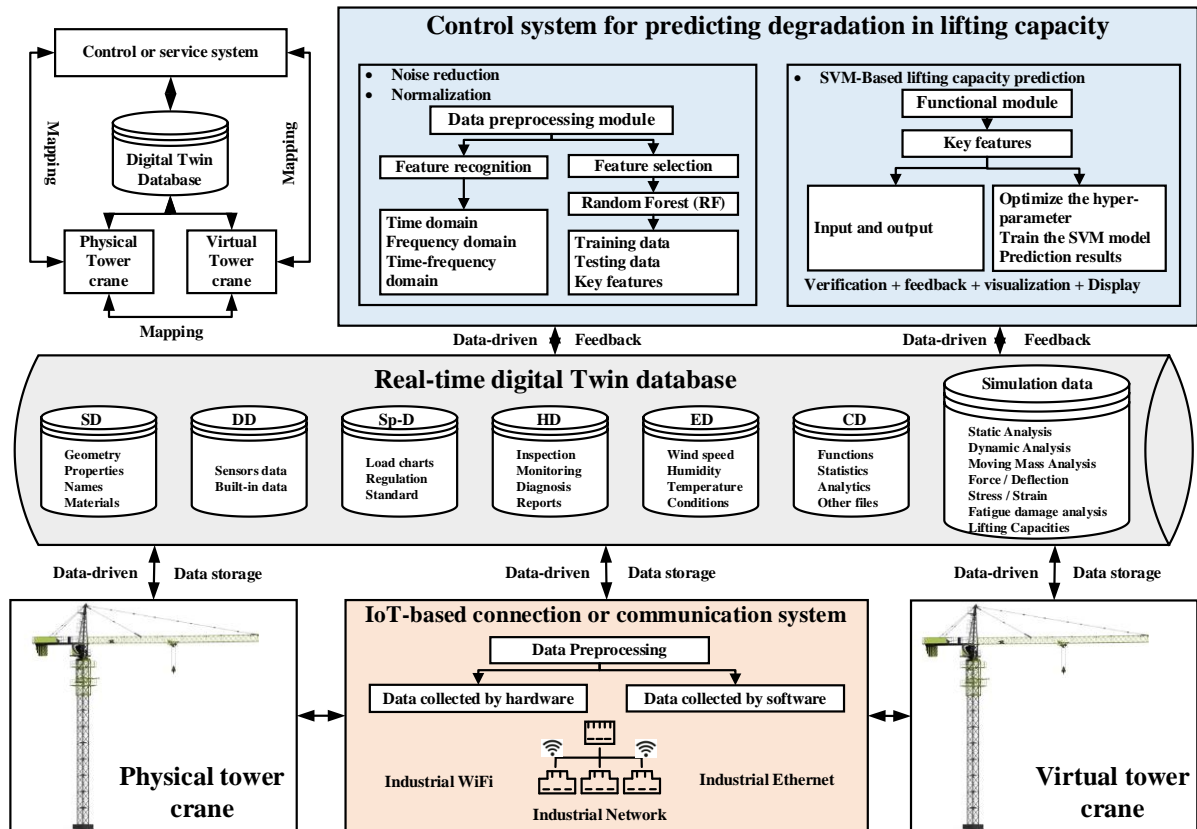
409 associations between sensory measurements (e.g., load magnitude, deflections, stress levels,
410 and cycle counts) and their corresponding damage indicators, indicating repetitive damage.

411 To ensure the reliability and accuracy of our predictive methodology, rigorous simulations
412 and real-world testing scenarios are conducted to validate its effectiveness. Detailed
413 discussions regarding the reliability and precision of our predictive approach can be found in
414 [Sections 4 and 5](#).

415 **4. A digital twin-driven model for degradation in cranes**

416 This study aims to develop a DTD model for predicting degradation in LC of aging tower
417 cranes, enabling intelligent decision-making, and providing feedback for the lifting operation.
418 As illustrated in [Fig. 4](#), a DTD model consists of five components described in [Section 3.1](#).
419 These components are integrated through the use of DT data. Multi-source, heterogeneous, and
420 real-time data are collected from a scaled-down prototype of a tower crane. This data is then
421 stored in the Firebase real-time database, serving as the foundation for prediction and decision-
422 making within the operational

423 system. The control system includes pre-processing and functional modules that utilize the
424 collected data for analysis and decision-making. The outcomes and insights generated by the
425 DTD model are fed back to the physical tower crane, improving its performance and
426 monitoring system. Additionally, the control system analyzes and visualizes the collected data,
427 providing operators, decision-makers, and management teams with valuable information for
428 monitoring degradation in tower cranes. In summary, the proposed DTD model facilitates the
429 interaction and fusion of its components to effectively monitor degradation in tower cranes,
430 enabling intelligent decision-making and feedback mechanisms for the lifting operation
431 process.



432

433 Fig. 4. A digital twin-driven model for predicting degradation in LC of aging tower cranes.

434 **4.1. Physical tower crane**

435 Tower cranes are tall structures commonly used in construction sites to lift heavy objects
 436 from the lifting position to target locations. Over time, these cranes experience degradation due
 437 to accumulating residual stresses caused by high-cycle and variable amplitude fatigue loads.
 438 Researchers, such as Jiang et al. [25], have explored two main areas of study to examine the
 439 structural mechanisms of tower cranes: (1) modeling and simulation and (2) scale models.

440 Modeling and simulation techniques, particularly the finite element method (FEM), have
 441 proven to be highly effective in analyzing the internal mechanism, dynamics, and structural
 442 behavior of tower cranes [46]. These approaches focus on critical aspects, design optimization,
 443 and safety risk performance. On the other hand, the scale model provides another avenue for
 444 studying the structural analysis and failure mechanism of tower cranes. Unlike numerical
 445 models, physical scale models allow for experimental testing of the crane's operation and
 446 control process. This enables easier detection of errors and deviations under various working
 447 conditions. He et al. [52] suggested that integrated modeling, simulation, and scale models can
 448 improve the structural analysis of tower cranes, predict failure modes, dynamic analysis, and
 449 operation processes. This previous research serves as the basis for the proposed DTD model,
 450 which employs integrated modeling, simulation, and scale modeling techniques in this study.

451 The scale model substitutes the large-size tower crane (STL420) structure. The construction
 452 of the scale model is based on the principle of similarity, as indicated in Eq. (3). The scale
 453 model contains the geometric attributes of all components, detailed in Table 1. The dimensions

454 of each part of the large-size tower crane are utilized to construct the corresponding scale-down
 455 components, as illustrated in Fig. 5. While the large-size tower crane is built using stainless
 456 steel, the scale model tower crane is fabricated using plastic materials. However, it is essential
 457 to note that the DTD model is developed based on the scale model. Consequently, during the
 458 FEM modeling process, the materials used for the scale model are defined as plastic. However,
 459 if one intends to apply our approach to a real crane, it is crucial to carefully consider the actual
 460 material and geometric properties. These factors play a pivotal role in addressing degradation-
 461 related issues effectively.

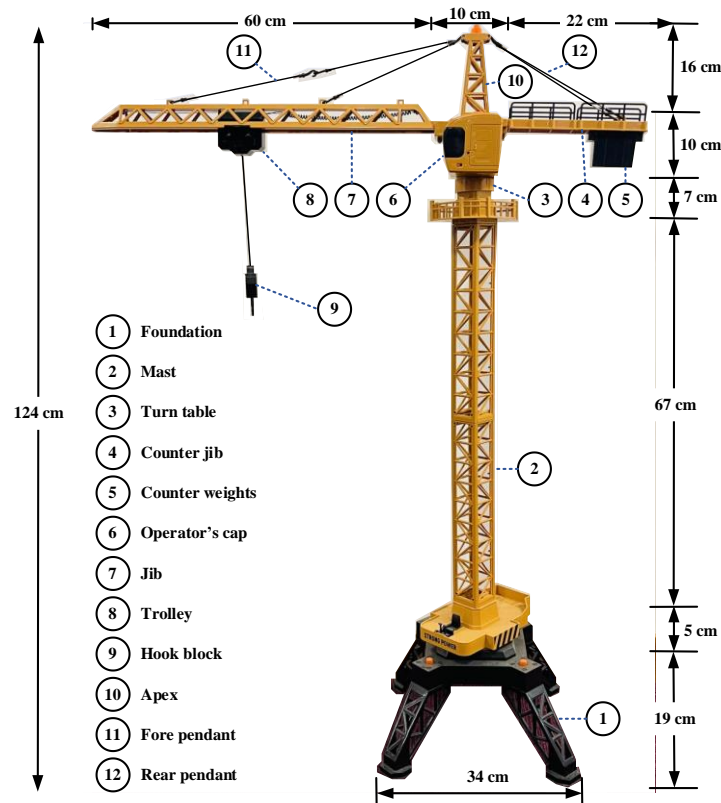
$$S_g = \frac{L_S}{L_R} = \frac{W_S}{W_R} = \frac{H_S}{H_R} \quad (3)$$

462 where S_g is the geometric similarity factor, S is the scale model, R is the real model, and L,
 463 W, and H are length, width, and height, respectively.

464 **Table 1.** Geometric similarity factors.

Structure	Scale size (L, W, H; cm)	Real size (L, W, H; cm)	Scale factor
Mast	(5.5, 5.5, 5.5)	(240, 240, 240)	1/43.6
Jib	L: 60	L: 6000	1/100
Counter jib	L: 22	L: 850	1/38.6
Rope	L: 122	L: 1650	1/13.5
Cross foundation	L*H: 34*19	L*H: 800*800	1/23.5*1/42.1
Load			
R (cm) 6000cm	500(gram)	1.089e+7 (gram)	1/21,772.4

465

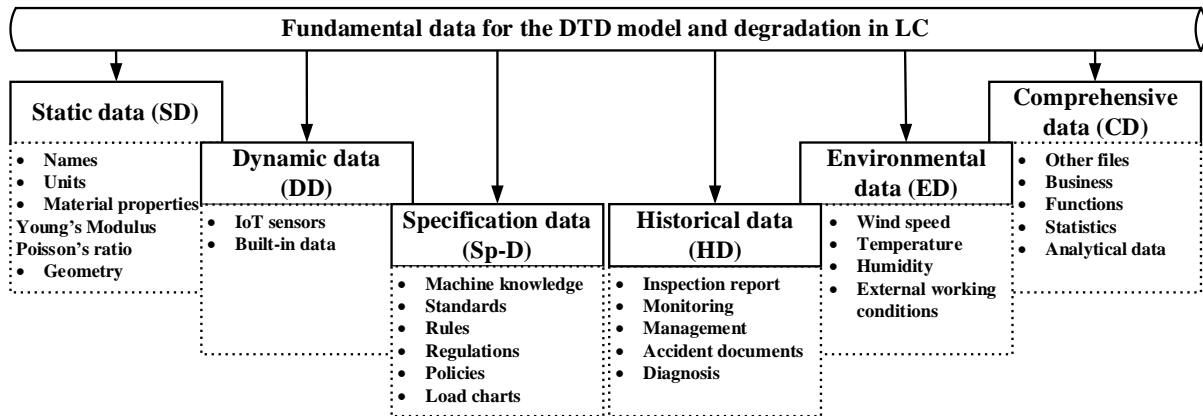


466

467 **Fig. 5.** Scale model of the tower crane and its components and dimensions.

468 **4.1.1. Fundamental data from the physical tower crane**

469 Data is the most essential and fundamental concept in developing a DTD model. In addition
 470 to sensors, other data types could be included to enhance the quality of a DTD model,
 471 particularly in the degradation scenario. As illustrated in **Fig. 6**, the tower crane generates
 472 multi-source heterogeneous data classified into six categories based on their type and nature:
 473 static, dynamic, specification, historical, environmental, and comprehensive data. Static data
 474 (SD) is data that does not change with time. Although SD does not directly influence
 475 degradation, it can affect quality if altered. In contrast, dynamic data (DD) varies with time.
 476 DD provides information about the crane's dynamics, lifting operation, degradation, and real-
 477 time operation status. DD is more important than other data types for developing the DTD
 478 model. As a result, it requires high accuracy, quality, and timeliness. DD consists of sensors
 479 and built-in data. Furthermore, specification data (Sp-D) includes knowledge, standards, and
 480 load charts. Historical data (HD) refers to data from inspections, monitoring, and maintenance
 481 reports during the service life. Besides this, environmental data (ED) refers to external working
 482 conditions, such as temperature, wind, and humidity. Finally, comprehensive data (CD) is
 483 additional data other than the previously mentioned data that provides essential and specific
 484 information to the DTD model for enhancing prediction and decision-making. In addition,
 485 simulation data is required for the DTD model, which we will explain in **Section 4.2**. Please
 486 note that we have developed a DTD model that utilizes real-time sensor data (DD data) and
 487 incorporates other data types in specific tasks. This integration enhances the quality and
 488 accuracy of assessing the degradation of tower cranes.



489

490 **Fig. 6.** Fundamental data for the DTD model and degradation.

491 **4.2. Virtual tower crane**

492 The virtual model of the tower crane serves as a simulation platform for analyzing its
 493 structure and operations. It accurately replicates the lifting operations of the actual crane,
 494 considering factors such as deterioration over time. The ABAQUS software is utilized to create
 495 a FEM model of the tower crane, enabling effective numerical simulations to determine the
 496 capacity of its structural components in terms of load and deflection. The analysis takes into
 497 account the working conditions of a scaled-down model, considering static, dynamic, and
 498 moving mass on the crane. All factors relevant to the lifting operations and degradation are
 499 incorporated as real-time external data in the virtual model.

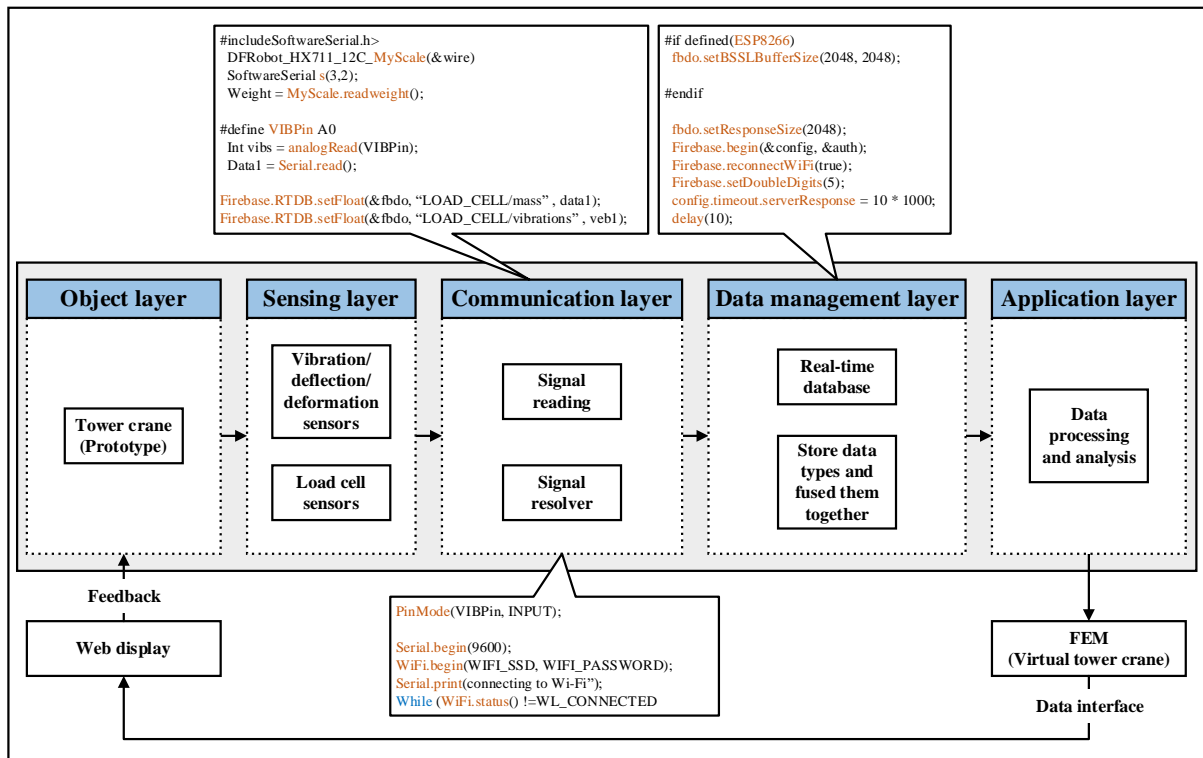
500 The tower crane is connected to its foundation through a baseplate and anchor bolts, which
 501 bear the bending moment and restrict movement in four nodal points and six degrees of
 502 freedom (DOF). The connection between the mast and jib section is assumed to be rigid, while
 503 the junction between the mast, tower cap, and pivoting support is consolidated. The jib and
 504 counter jib are hinged to the mast. Finite element analysis (FEA) is performed using various
 505 loads, including dead, service, wind, and concentrated loads. This analysis helps determine the
 506 LC of the tower crane by examining a force/deflection or stress/strain curve. Additionally, a
 507 fatigue damage accumulation analysis is conducted to assess the rate of damage and
 508 degradation over a 70-year period. The ABAQUS software stores all relevant information
 509 about the lifting operation, including component geometry, mechanical data, operational
 510 process, and environmental conditions. Finally, the degradation rate is integrated and used in
 511 conjunction with real-time sensor data in the control system of the DTD model to predict
 512 degradation in the LC of a tower crane, as explained in [Section 3.3](#).

513 **4.3. IoT-based connection and dataflow**

514 The Internet of Things (IoT) system monitors the real-time status of a physical tower crane.
 515 In the DTD model, the IoT plays a crucial role as both a source of real-time data and a source
 516 of mechanism for transferring that data. As depicted in [Fig. 7](#), this system is organized into five
 517 layers: the object, sensing, communication, data management, and application.

518 The object layer consists of a scaled-down prototype of the tower crane, which generates
 519 real-time data through sensors, as discussed in [Section 4.1.1](#). The sensing layer incorporates

520 various sensors such as vibration, deformation, deflection, and load cell sensors. These sensors
 521 are primarily used for data acquisition and control via different interfaces, such as OPC-UA.
 522 The communication layer collects and transfers all types of data using serial port converters
 523 and communication modules. It facilitates the seamless flow of data within the IoT system. The
 524 data management layer includes a database that stores and integrates essential data translated
 525 into different formats. This layer supports functions like perception, knowledge, and algorithms
 526 to assist the application layer. Finally, the application layer is the fundamental component of
 527 the IoT system. It allows communications between the OPC interface and the server. This layer
 528 is for cleaning, association, mining, fusion, and analysis across all subsystems.



529
 530 **Fig. 7.** IoT system and dataflow.

531 **4.4. Real-time digital twin database**

532 To effectively extract critical features related to LC degradation, advanced data conversion
 533 technology is necessary. This technology enables the integration and manipulation of sensor
 534 data, fundamental data, and simulation data. The diverse nature of LC degradation necessitates
 535 using multiple data formats and sources, each with its unique characteristics.

536 To address these challenges, a Firebase real-time database is employed. This database
 537 encompasses all aspects of LC deterioration, providing a comprehensive solution. By
 538 leveraging the capabilities of Firebase, the system can handle the complexities arising from
 539 various factors influencing LC degradation and the heterogeneous nature of the data involved.

540 **4.5. Control system for predicting degradation**

541 Traditionally, operators and workers are mainly responsible for monitoring and controlling
 542 lifting operations. A qualified individual follows the manufacturer's specifications and

543 directions to ensure a safe lifting operation. The manufacturer's rated loads for a crane are based
544 on ideal conditions. If an individual adheres to the manufacturer's loads for an extended period,
545 the tower crane may be damaged. Therefore, a hybrid and real-time approach is required to
546 illustrate the current status, predict the LC of a tower crane, and present the predicted LC in
547 updated load charts and graphs. The control system is thus designed and comprises (1) pre-
548 processing and (2) functional modules.

549 The pre-processing module handles data monitoring, analysis, and evaluation for LC
550 prediction. Sensor signals typically contain noise, which can adversely affect the accuracy of
551 LC prediction. Appropriate de-noising methods are commonly employed to mitigate this issue
552 and enhance the precision of the predictions. However, in the context of this study, unique de-
553 noising methods were not utilized as they were not directly relevant to the Firebase database.
554 Instead, we employed two different steps to denoise the raw data. 1) We utilized a
555 communication protocol or interface, such as a Universal Asynchronous Receiver/Transmitter
556 (UART), to transfer data from ESP8266 to an Arduino. This step helped in reducing noise
557 during the data transfer process. 2) We applied the Power Exponential Denoising (PED)
558 method specifically for the load cell. This technique effectively reduced the noise present in
559 the load cell data, further enhancing the accuracy of the predictions. Moreover, data
560 normalization is performed within this module. A feature recognition technique such as time-
561 domain is applied to extract information from the signals. Subsequently, a features selection
562 method is utilized to identify the most relevant features. The dataset is then divided into training
563 and testing datasets for further processing.

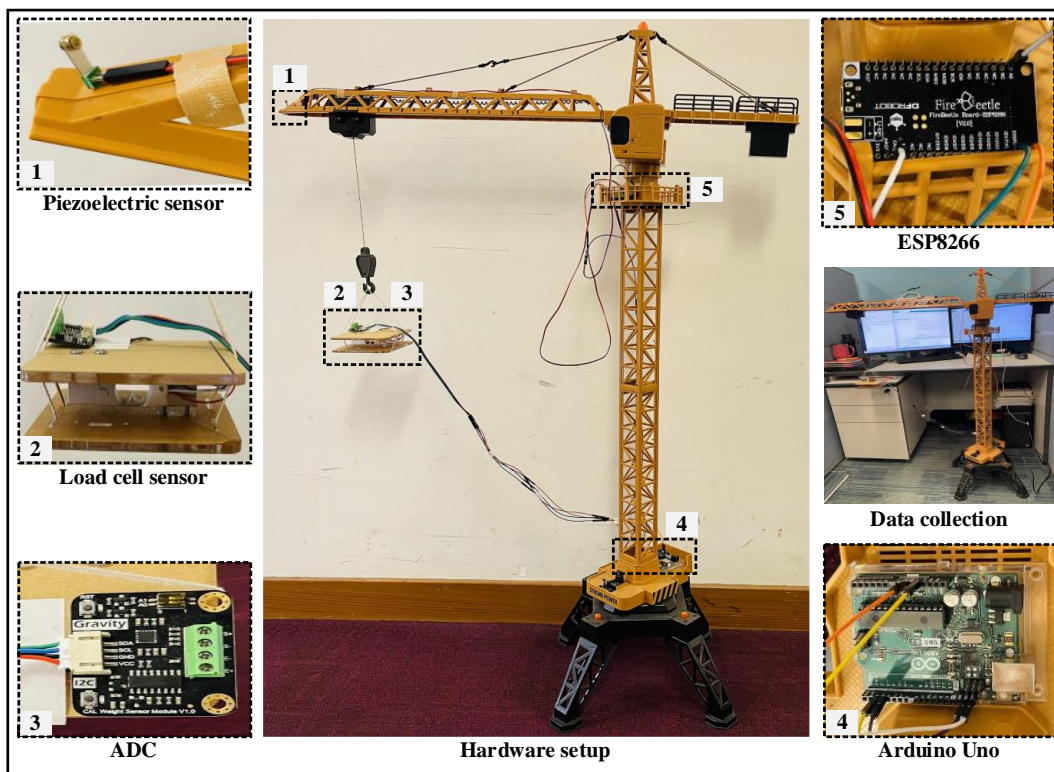
564 In the functional module, important features influencing the LC of the tower crane are
565 selected. Real-time sensor data is utilized by the DTD technique to assess the current condition
566 of the lifting operation. However, real-time data alone cannot predict the degradation rate of
567 LC or how quickly the LC decreases over time. To address this limitation, FEA is conducted
568 to evaluate fatigue damage accumulation and degradation. The degradation rate obtained from
569 FEA is incorporated and manipulated in the database, as described in [Section 3](#). An appropriate
570 machine learning (ML) model is employed to accurately predict degradation in the LC of the
571 tower crane. The high-precision findings are then fed back to the physical tower crane,
572 minimizing unexpected failures and damages while enhancing monitoring capabilities and the
573 overall safety of the lifting operation.

574 **5. Case study**

575 In this study, we utilized a scaled-down prototype of the “STL420” tower crane to evaluate
576 the accuracy, effectiveness, and applicability of the proposed DTD model. Although the
577 prototype has some flaws, none of them hinder our research objectives. For instance, the shape
578 of the foundation/baseplate differs from the actual crane, but the bending moment is restrained
579 to four nodes and six DOFs, mirroring real cranes. Furthermore, the prototype's mast consists
580 of only two sections, whereas the mast of the actual crane has more sections, varying in height.
581 However, this discrepancy does not impact our model since we do not consider critical
582 components or joint failures in the degradation analysis. Finally, although the slewing unit and
583 climbing frame differ in shape, their functions remain identical.

584 **5.1. Physical hardware setup**

585 The scaled-down prototype is equipped with two direct-current (DC) motors that enable
586 horizontal rotation in both clockwise and counter-clockwise directions, trolley movement
587 inward and outward, as well as loading and unloading operations through a remote control.
588 Additionally, as shown in Fig. 8, two sensors, namely a load cell and a piezoelectric sensor,
589 are installed on the prototype to measure the load and deflection. The piezoelectric sensor is
590 positioned at the end of the jib where deflection is higher, while the load cell is mounted
591 beneath the hook. The load cell is connected to the HX711 ADC, Arduino Uno, and NodeMCU
592 ESP8266 Wi-Fi module for data collection and storage. This configuration enables
593 bidirectional communication between the physical and virtual cranes.



594

595 Fig. 8. Physical hardware setup.

596 **5.2. DTD model experimental platform**

597 The main objective of the experimental platform is to conduct lifting operations. A scaled
598 model was constructed to achieve this, and lifting operations were carried out to generate and
599 collect data. In order to measure loads and deflection, a load cell and piezoelectric sensors were
600 installed. Additionally, the actual crane provided three load charts corresponding to
601 counterweights of 12, 18, and 24 tons, along with four jibs of lengths of 30m, 40m, 50m, and
602 60m attached to the mast. Following the principle of similarity, we utilized a scaled model with
603 a 60-meter jib and 24 tons of counterweights. The load chart for the actual crane is presented
604 in Table 2. Applying the scale factor, the load chart for the scaled-down tower crane is shown
605 in Table 3.

606 Fig. 9 illustrates the scale model used, which features a jib length of 60 cm and a trolley
607 movement limited to a range of 15 cm to 50 cm. To determine the loads for different lifting
608 radii, we applied scaled-down factors and marked the corresponding radii on the jib using a
609 black marker, as shown in Fig. 8. Each marked lifting radius was then assigned a calculated
610 load. For each point load, three operations were performed to measure load and deflection: (1)
611 loading and unloading, (2) clockwise and counterclockwise rotation, and (3) rotation while
612 loading and unloading. Each point load experiment lasted 10 minutes, during which we
613 completed all three operations. Three tests were conducted for each point load, and the results
614 were averaged. This generated a dataset consisting of 54 experiments conducted at 18 different
615 locations. Simultaneously, the virtual environment simulated the hoisting process. The load
616 values calculated from Table 3 were used to establish the relationship between stress/strain or
617 load/deflection. As discussed in Section 3, residual stresses accumulate when loads are applied
618 cyclically over several years, leading to degradation. Therefore, we calculated seven
619 degradation indices for each load, representing 10, 20, 30, 40, 50, 60, and 70 years. Finally, the
620 degradation rates obtained from the degradation indices were combined and manipulated to
621 real-time sensor data to predict the degradation in LC of the tower crane; a detailed process
622 was explained in Section 3.3.

623 Table 2. A load chart of the actual tower crane.

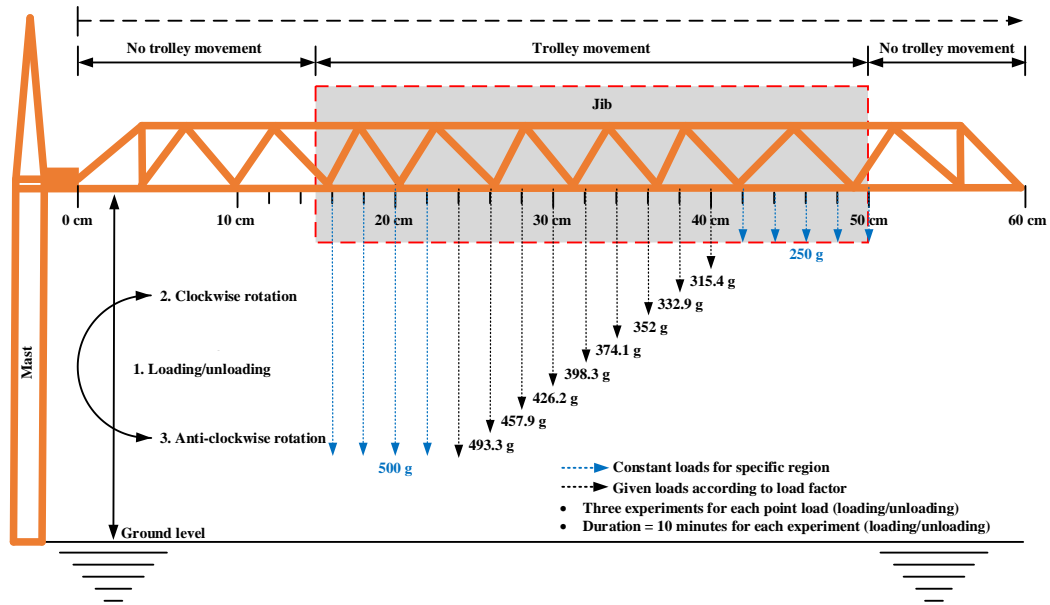
Jib (m)	LC _M ax (t)	Lifting radius (m)														
		20	22	24	26	28	30	32	34	36	38	40	45	50	55	60
60	12	12.0	12.0	12.0	11.8	10.9	10.2	9.56	8.98	8.45	7.99	7.57	6.6	5.9	5.3	4.9
		0	0	0	4	9	3						8	7	8	0
50	18	18.0	18.0	17.2	15.8	14.7	13.7	12.8	12.0	11.3	10.7	10.1	8.9	8.0		
		0	0	6	9	2	0	1	2	3	0	4	5	0		
40	24	22.6	20.5	18.7	17.2	15.9	14.7	13.7	12.8	12.1	11.4	10.8				
		6	2	4	3	4	3	5	9	2	3	5				
30	24	23.2	21.0	19.2	17.7	16.3	15.2									
		9	9	5	0	6	5									

624

625 Table 3. A load chart of the scale-down tower crane prototype.

Jib (c m)	LC _M ax (g)	Lifting radius (cm)														
		20	22	24	26	28	30	32	34	36	38	40	45	50	55	60
60	500	500.	500.	500.	493.	457.	426.	398.	374.	352.	332.	315.	278.	248.	224.	204.
		0	0	0	3	9	2	3	1	0	9	4	3	7	1	1
50	750	750.	750.	719.	662.	613.	570.	533.	500.	472.	445.	422.	372.	333.		
		0	0	1	0	3	8	7	8	0	8	5	9	3		
40	100	944.	855.	780.	717.	664.	613.	572.	537.	505.	476.	452.				
		0	1	0	8	9	1	7	9	0	0	2	0			
30	100	970.	878.	802.	737.	681.	635.									
		0	4	7	0	5	6	4								

626



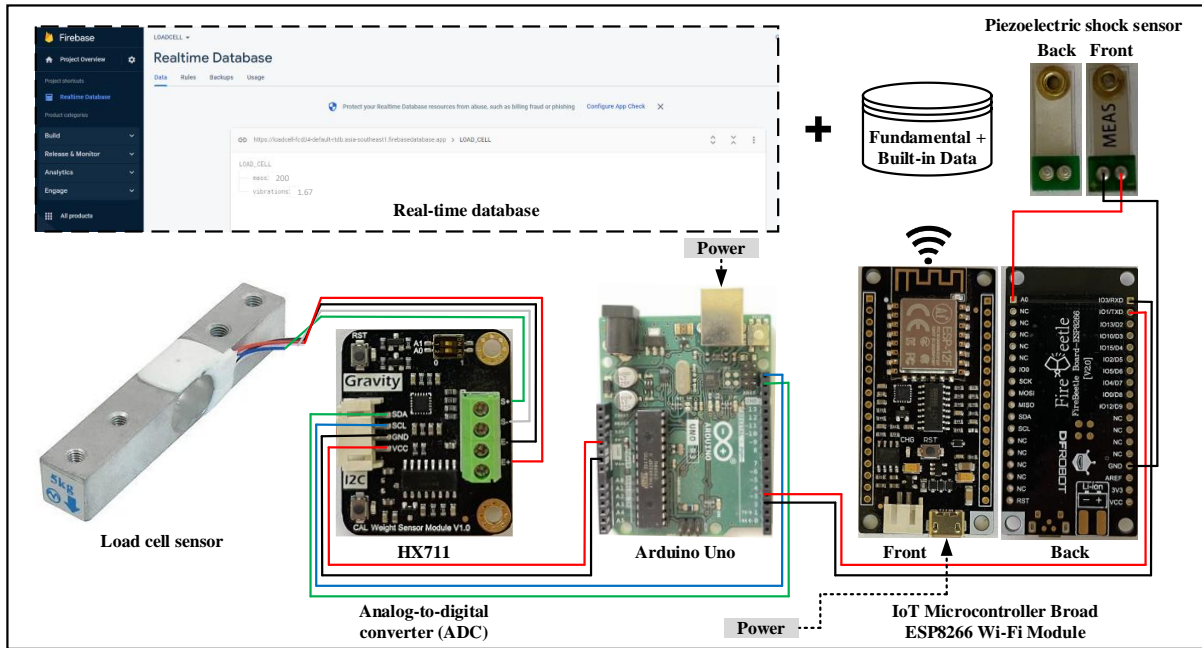
627

628 Fig. 9. Experimental platform for the lifting operations.

629 **5.3. Data collection**

630 Fig. 10 illustrates the connection of the load cell and piezoelectric sensors to the analog
 631 input pins of an Arduino Uno for data collection and pre-processing. Initially, the raw data is
 632 measured as a voltage ranging from 0 to 5 volts at a frequency of 250 hertz. To convert the raw
 633 data into integer values between 0 and 1023, a 10-bit HX711 ADC is employed. Subsequently,
 634 the load and deformation/deflection data undergo a smoothing process, where an average of 20
 635 measurements is taken for three different weights (100g, 200g, and 300g) to enhance data
 636 accuracy and calibrate the measurements. Finally, the smoothed data is multiplied by a
 637 predetermined conversion factor to obtain measurements for load (in grams) and
 638 deflection/deformation (in millimeters).

639 Additionally, the data collection module encompasses SD, Sp-D, HD, ED, and CD at
 640 various stages of the DTD model. For example, when modeling a virtual tower crane, geometric
 641 and material properties are taken into account. In the case of HD, a diagnosis report is examined
 642 to assess the precision and accuracy of deterioration, considering the impact of repair and
 643 replacement procedures on degradation. Furthermore, environmental conditions such as wind
 644 load, temperature, humidity, and others are considered during finite-element (FEA) and fatigue
 645 damage accumulation analyses.



646

647 **Fig. 10.** A circuit diagram or IoT system for data collection.

648 **5.4. Data transmission to the cloud**

649 The Arduino communicates the load and vibration/deflection/deformation data to an
 650 ESP8266 module through a serial port. The transmission via serial takes approximately 37
 651 milliseconds, as determined through measurements. To optimize the usage of transmission
 652 bandwidth, the average measurements are programmed to be sent every second. This ensures
 653 reliable data transmission between the sensors and the cloud gateway. When an average
 654 measurement is obtained, the cloud gateway converts the values into JSON format and includes
 655 a timestamp.

656 **5.5.FE analysis or simulation environment**

657 The objective of simulation within a DTD model is to replicate a specific process or
 658 operation within a virtual environment. ABAQUS software is utilized to construct a finite-
 659 element model (FEM) for this purpose. As shown in **Fig. 11**, a non-linear static analysis is
 660 conducted on a crane structure, considering both material and geometric nonlinearity.
 661 Variations in boundary conditions, particularly for the boom structure, are also taken into
 662 account. The load combination comprises a dead, wind, and lifting load. The equivalent static
 663 load is determined by multiplying the static load by a dynamic load coefficient. In the virtual
 664 environment, the yield and ultimate strength of the crane material are considered. While the
 665 data exhibit a similar pattern, the magnitudes may differ. The crane structure undergoes
 666 vibration/deflection when subjected to cyclic loading. Prolonged exposure to such loading and
 667 vibration leads to degraded capacity due to the accumulation of residual stresses. We aim to
 668 quantify and incorporate the degradation rate into real-time data, thereby reducing the
 669 magnitude and aligning the real-time sensor data with the simulation data.

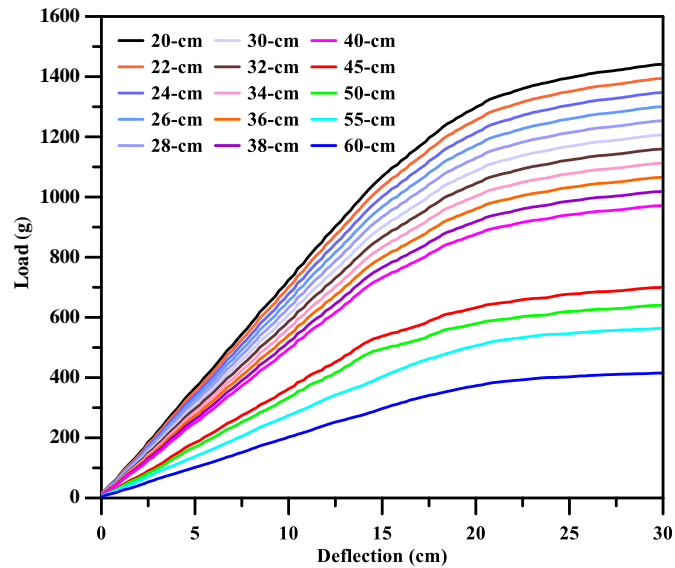


Fig. 11. Non-linear static analysis of the tower crane.

670

671

672 5.6. Control system and synchronization

673 The ESP8266 devices manage the cloud gateway and the control module, which are
 674 connected to the cloud database. Real-time data synchronization is achieved through the use of
 675 WebSockets, enabling communication between physical and virtual cranes in both directions.
 676 The Firebase real-time database stores sensor data and control codes in this study. The cloud
 677 gateway transmits structured data to the real-time database every second. To facilitate
 678 backward testing and analysis, each simulated value is stored in the historical database. The
 679 JSON objects consist of six layers of nodes, which is advantageous for training machine
 680 learning (ML) modules due to variations in sensor data features across operational nodes.
 681 Consequently, a machine learning-based classification engine can effectively utilize this
 682 historical data.

683 5.6.1. Historical data hosting and computation engine

684 While establishing a direct relationship between load, deflection, degradation rate, and LC
 685 poses challenges, a machine learning-based classification engine can effectively utilize
 686 historical data. The training and testing process relies on data collected during the idle state,
 687 ensuring that operation only commences under safe conditions. Initially, the sensory data is
 688 pre-processed by grouping values into 10-second intervals. For each sensor, a rolling standard
 689 deviation is calculated to generate additional features for ML. The most recent timestamp is
 690 used for the aggregated data, and the state with the highest count is considered the congregated
 691 state. Delta time is disregarded as it does not contribute to the learning engine. A one-class
 692 categorization method based on similarity is implemented, utilizing a support vector machine
 693 (SVM) model. The model learns the characteristics of typical scenarios and predicts whether
 694 incoming input deviates from these specific occurrences. Finally, the dataset is validated by
 695 analyzing the model's accuracy using k-fold cross-validation. To simplify matters, a control
 696 system is divided into two modules: pre-processing and functional.

697 5.6.2. Preprocessing module

698 The pre-processing module monitors, analyzes, and evaluates real-time data related to the
699 lifting operation. The raw or sensory data contains crucial information that influences the LC.
700 Feature recognition techniques, such as time-domain, are employed to extract the relevant
701 features from the signal. Key features for the LC, including Load (g), deflection (mm), boom
702 length (cm), lifting radius (cm), counterweight (g), and degradation rate, are determined as the
703 primary factors. While considering all parameters that affect degradation and LC is
704 challenging, incorporating optimal parameters can enhance prediction accuracy, as noted by
705 Roysson et al. [73]. The random forest (RF) model is employed to select the features after
706 feature recognition. RF combines the CART tree and random subspace, where a CART tree
707 consists of decision nodes, leaf nodes, and root nodes. Each tree is constructed using the
708 independent random sample approach. The bagging or bootstrap technique creates subsets, and
709 a random subset of feature attributes is chosen based on a specific criterion. RF generally
710 outperforms single decision trees due to the voting-based selection of outcomes from multiple
711 trees. In this study, the essential features are selected using different n-estimator
712 hyperparameters, namely 100, 250, 500, 750, and 1000. The dataset is divided into 70%
713 training and 30% testing sets. The importance values for the Load (g), deflection (mm), boom
714 length (cm), lifting radius (cm), counterweight (g), and degradation rate are 0.37, 0.34, 0.13,
715 0.14, 0.0, and 0.2, respectively. In this case, the counterweight importance is zero as it remains
716 constant during lifting. Table 4 presents the errors and R² values obtained from the RF feature
717 selection process.

718 **Table 4:** Errors and R² values for the random forest (RF).

Model	Hyperparameter	Trees	Mean absolute error (MAE)	Root mean square error (RMSE)	Mean absolute percentage error (MAPE)	R- square (R ²)
Random forest (RF)	n-estimator	100	0.174	0.232	2.1%	0.997
		250	0.168	0.227	2.1%	0.997
		500	0.166	0.225	2.0%	0.997
		750	0.169	0.226	2.1%	0.997
		1000	0.168	0.225	2.1%	0.977

719

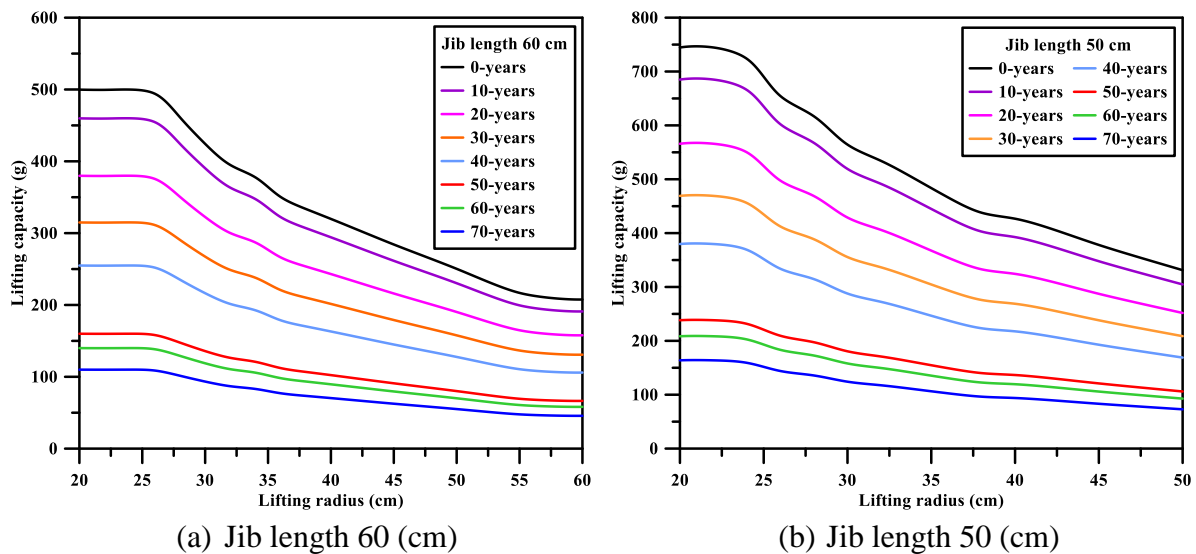
720 **5.6.3. Functional module**

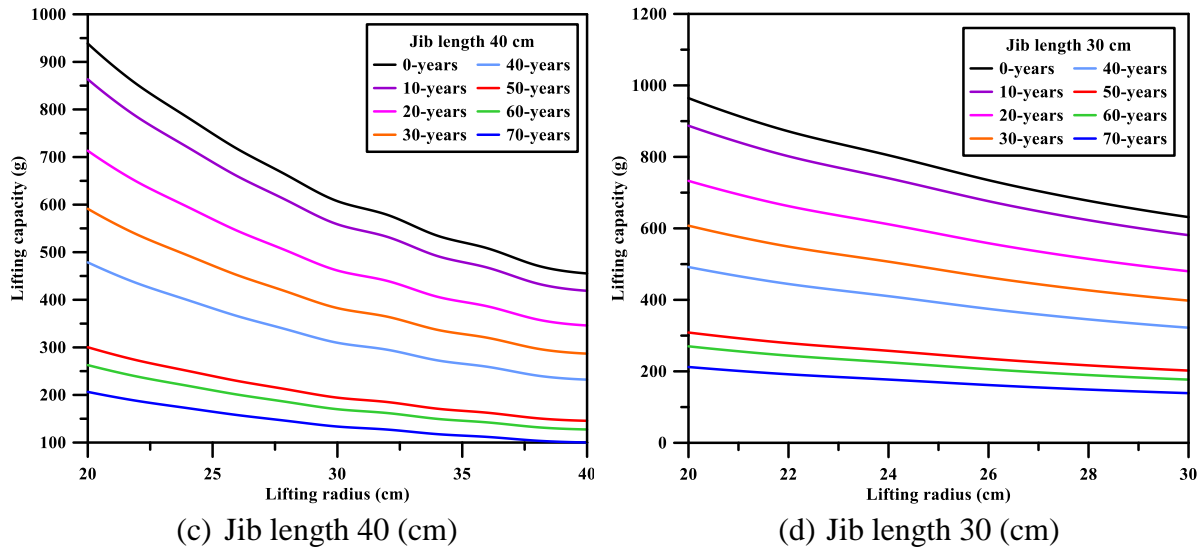
721 Predicting the complex and non-linear problems of LC and its degradation using traditional
722 mathematical models is challenging due to their multi-variable nature. In this regard, machine
723 learning (ML) provides significant advantages for accurate prediction. The SVM model is
724 employed to predict degradation in LC, as it excels in handling high-dimensional data with
725 distinct margins and scattered data points. To ensure the model's accuracy, the authors utilized
726 a 70% dataset for training and reserved 30% for testing. The input variables consist of Load
727 (g), deflection (mm), boom length (cm), lifting radius (cm), counterweight (g), and degradation
728 rate, while the output variable is lifting capacity (g). Evaluation of the model is performed

729 based on two criteria: mean square error (MSE) and coefficient of determination (R^2). MSE
 730 measures the average squared difference between the predicted values and the actual values,
 731 reflecting the prediction error. On the other hand, R^2 represents the proportion of the variance
 732 in the dependent variable (LC) that can be explained by the independent variables (load,
 733 deflection, boom length, lifting radius, counterweight, and degradation rate). R^2 values range
 734 between 0 and 1, with values closer to 1 indicating a better performance of the prediction model
 735 and smaller prediction errors. Smaller MSE values and R^2 values closer to 1 indicate smaller
 736 prediction errors and better performance of the prediction model. In this study, the MSE and
 737 R^2 values are reported as 0.2253 and 0.9973, respectively. These values demonstrate that the
 738 SVM model is a good fit for the data and analysis, as it accurately predicts the outcomes. It is
 739 worth noting that high-quality, consistent, and reliable sensor data contribute to achieving high
 740 R^2 values.

741 The evaluation of the DTD model reveals its flexibility and accuracy in predicting
 742 degradation in complex machines such as cranes. The degradation rate is integrated into the
 743 control system, calculated based on fatigue damage accumulation and FE analysis. Fig. 12
 744 illustrates the predicted degradation in LC for a tower crane, where the predicted results of LC
 745 (g) are plotted against the lifting radius (cm) for a boom length of 60cm. The predicted results
 746 are scaled for boom lengths of 30cm, 40cm, and 50cm by multiplying them with a scale factor.

747 Table 5 displays the predicted load charts for a prototype crane, considering 0 years and
 748 70 years of operation. The high-precision findings obtained from the model are fed back to the
 749 physical tower cranes. Moreover, Table 6 demonstrates that when the load chart of the
 750 prototype is scaled using a scale factor, it matches the load chart of the actual tower crane. By
 751 calculating the degradation rate and continuously updating the load chart over the service life
 752 of the tower crane, operators, management, or decision-making teams can make informed
 753 decisions regarding crane operations and maintenance planning, considering more accurate LC
 754 information.





755 Fig. 12. Predicted LC of the tower crane for 70 years: (a) Jib length 60 cm, (b) Jib length 50
 756 cm, (c) Jib length 40 cm, and (d) Jib length 30 cm.

757 Table 5. Predicted load charts (gram) for the prototype for 0 and 70 years.

Jib (cm)	Lifting radius (cm)														
	20	22	24	26	28	30	32	34	36	38	40	45	50	55	60
60	499.	499.	499.	494.	461.	424.	394.	377.	350.	333.	319.	284.	250.	216.	207.
50	744.	744.	723.	654.	616.	564.	534.	501.	466.	437.	426.	378.	331.		
40	938.	851.	783.	716.	661.	607.	578.	534.	508.	471.	455.				
30	964.	871.	804.	734.	677.	631.									

Jib (cm)	Lifting radius (cm)														
	20	22	24	26	28	30	32	34	36	38	40	45	50	55	60
60	110.	109.	110.	108.	101.	93.3	86.9	83.1	77.1	73.4	70.4	62.5	55.1	47.7	45.7
50	163.	163.	159.	144.	135.	124.	117.	110.	102.	96.3	93.9	83.2	72.9		
40	206.	187.	172.	157.	145.	133.	127.	117.	111.	103.	100.				
30	212.	191.	177.	161.	149.	138.									

758

759 Table 6. Predicted load charts (ton) for the real tower crane based on a scale factor for 0 and
 760 70 years.

For 0-years:															
Jib (m)	Lifting radius (m)														
	20	22	24	26	28	30	32	34	36	38	40	45	50	55	60
60	11.9	11.9	11.9	11.8	11.0	10.1	9.4	9.0	8.4	8.0	7.6	6.8	6.0	5.2	4.9
50	17.8	17.8	17.3	15.7	14.8	13.5	12.8	12.0	11.1	10.5	10.2	9.0	7.9		
40	22.5	20.4	18.7	17.2	15.8	14.5	13.8	12.8	12.2	11.3	10.9				
30	23.1	20.9	19.3	17.6	16.2	15.1									

For 70-years:															
---------------	--	--	--	--	--	--	--	--	--	--	--	--	--	--	--

Jib (m)	Lifting radius (m)														
	20	22	24	26	28	30	32	34	36	38	40	45	50	55	60
60	2.6	2.6	2.6	2.6	2.4	2.2	2.1	2.0	1.9	1.8	1.7	1.5	1.3	1.1	1.1
50	3.9	3.9	3.8	3.5	3.3	3.0	2.8	2.6	2.5	2.3	2.3	2.0	1.7		
40	5.0	4.5	4.1	3.8	3.5	3.2	3.1	2.8	2.7	2.5	2.4				
30	5.1	4.6	4.2	3.9	3.6	3.3									

761

762 5.7. Validation

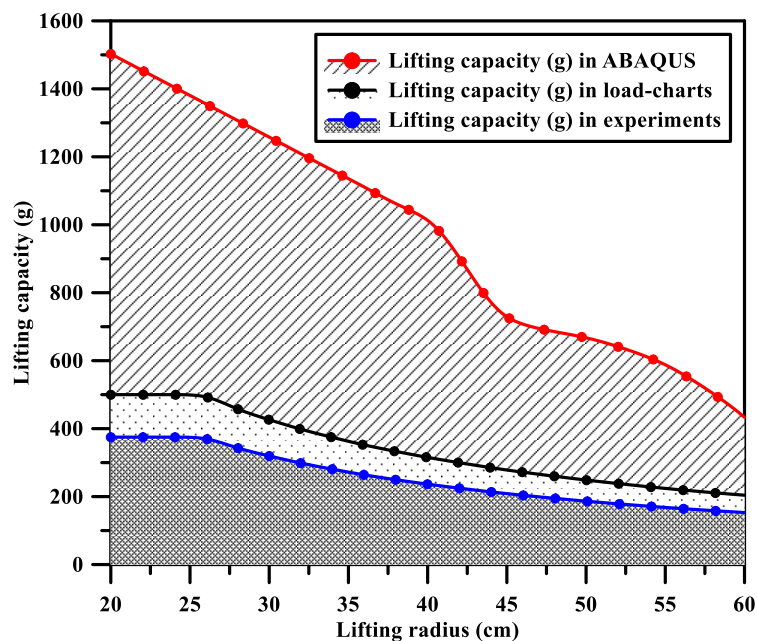
763 In order to account for the inherent unpredictability and variability in the experiment, a
764 DTD model is applied to evaluate the degradation in LC of a tower crane using sample data.
765 To validate the accuracy of the DTD model, a k-fold cross-validation approach is employed.
766 The sample data is trained and predicted using SVM with k-5 cross-validation. The predictions
767 demonstrate a high accuracy of 0.97 (R^2), comparable to that of a typical SVM model.
768 Therefore, the proposed DTD model proves to be convenient, efficient, and based on real-time
769 data, providing reliable results for predicting degradation in LC.

770 6. Discussion

771 This section presents the results of the DTD model, including the physical tower crane,
772 virtual tower crane, IoT-based connection, data storage, and control system. Firstly, a scale-
773 down tower crane prototype equipped with load cell and piezoelectric sensors was utilized to
774 collect load and deflection data. The prototype also generated fundamental data considered at
775 different stages of a DTD model. Previous approaches, such as analytical methods [67], non-
776 destructive technologies [74], and numerical simulations [60, 65, 69], necessitated the use of
777 hypothetical and artificial models to conduct experiments and determine failure mechanisms.
778 Whereas data-driven models [23, 75] are data-intensive and need data for at least one year.
779 Following the principle of similarity, the scaled model served as a substitute for the actual
780 tower crane, enabling a realistic assessment of structural analysis, failure mechanism,
781 dynamics, operation, and control process. For instance, Jiang et al. [25] used a tower crane
782 prototype to investigate stability analysis and hoisting safety, while He et al. [52] used a
783 prototype to study the impact of wind on cranes. The proposed DTD model offers several
784 benefits over the existing methods, as it integrates a scaled model, sensors, and simulation data
785 to predict degradation in LC.

786 Next, in the DTD model, the primary aim of the simulation is to replicate the lifting
787 operation within a virtual environment. Consequently, adjustments, edits, updates, and
788 calibrations can be made to the simulation of the virtual body until it aligns with the physical
789 body in terms of LC. In our study, the load and deflection values were consistent between the
790 physical and virtual cranes. However, there was a slight disparity in the material capacities of
791 the physical and virtual bodies due to safety considerations on the construction site and
792 experimental platform, as depicted in Fig. 13. A non-linear static analysis using ABAQUS was
793 employed on a scaled model to calculate the material capacity as load/deflection, unlike load
794 charts provided by manufacturing companies based on material properties. Nevertheless, a
795 safety margin was incorporated into the construction or experimental platform to mitigate
796 unforeseen failures. The collisions observed between the physical and virtual LC were

797 attributed to a factor of safety (FOS). In Fig. 13, the region under the blue line represents a
 798 safe/working zone, while it becomes a hazardous zone if it exceeds the blue line. The area
 799 under the red line denotes a damage zone, and beyond the red line indicates a failure zone,
 800 indicated in white. Although the physical and virtual data exhibited similar patterns, there were
 801 discrepancies in magnitudes. To address this, we quantified the degradation rate and integrated
 802 it with real-time data to reduce the magnitude and align the data from sensors and simulation
 803 [46, 61, 64, 65, 68, 76]. A similar approach was employed by Yang et al. [37], who multiplied
 804 wear data with a field-measurable precision index value. In summary, we developed a DTD
 805 model based on working loads and deflection. As working loads and deflection persist over
 806 several years, the material capacity will degrade due to residual stresses. Therefore, we
 807 calculated the residual stresses and incorporated them with operational values to predict
 808 degradation.



809

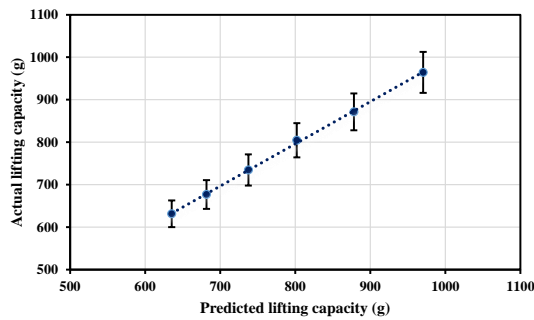
810 **Fig. 13.** Physical and virtual cranes load comparison and their zones.

811 Likewise, in a DTD model, the data flow is automated and stored in a real-time database.
 812 There is a bidirectional connection established between the virtual and physical cranes, unlike
 813 digital shadow, which lacks this capability [77]. Additionally, LC and degradation are
 814 influenced by various factors and described in different data formats with diverse and
 815 heterogeneous characteristics. Therefore, advanced data conversion technology is necessary to
 816 integrate and manipulate data from sensors, simulations, and fundamental sources in order to
 817 extract features relevant to LC and degradation. Moreover, all components of the proposed
 818 DTD model are integrated and mapped to detect and respond to real-time changes in the
 819 physical space, as well as to provide feedback to the control system. The secure connection and
 820 data transmission between the physical and virtual cranes, and vice versa, are also considered.

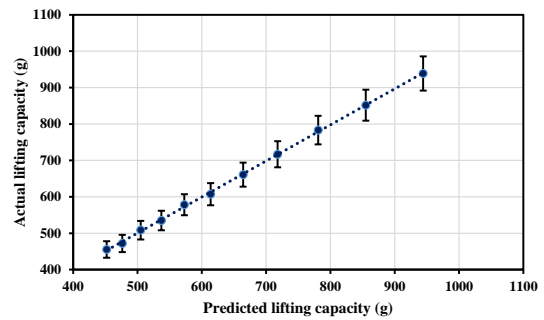
821 Lastly, the control system plays a crucial role in the DTD model by utilizing real-time data
 822 to predict degradation in LC. It operates in a hybrid mode and serves as the fundamental
 823 component responsible for analyzing and visualizing real-time changes, making informed

824 decisions, and providing feedback for further improvements. The control system performs
 825 essential tasks such as pre-processing, noise reduction, calibration, normalization, and raw and
 826 real-time data evaluation. It also incorporates feature recognition and selection. In DT
 827 technologies, it is crucial for the sensor and simulation data to align and encompass optimal
 828 parameters related to specific activities, as this integration and adjustment enhance prediction
 829 accuracy. In our study, we predicted the degradation in LC of a tower crane over a period of
 830 70 years, presenting the results through graphs and load charts. Additionally, we utilized
 831 scaling and similarity factors to forecast degradation for various scaled-down jib lengths,
 832 including 30cm, 40cm, 50cm, and 60cm. In a related study, Roysson et al. [73] employed ANN
 833 for predicting the LC of a mobile crane, but the average deviation between the actual and
 834 predicted LC was 1.3. In our case, however, the average deviation between the actual and
 835 predicted LC is 2.6, indicating a higher level of deviation compared to previous research. This
 836 disparity can be attributed to our utilization of sensors, simulations, degradation rates, and six
 837 input parameters. In contrast, they relied on data solely from load charts and only three input
 838 parameters.

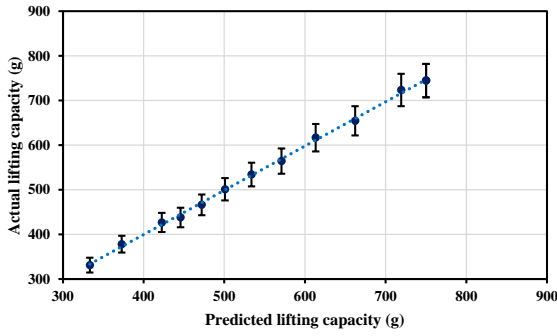
839 Similarly, Yang et al. [37] employed a DTD approach to predict performance degradation
 840 in the transmission unit of a CNC machine tool, achieving an average error of 4.33%. Our study
 841 utilized Mean Squared Error (MSE) and R-squared (R^2) as evaluation criteria for the DTD
 842 model. The prediction model yielded an MSE of 0.2253 and an R^2 of 0.9973. We compared
 843 the results with a traditional SVM model to validate our model, and the average prediction
 844 accuracy was nearly 99%. As illustrated in Fig. 14, the average deviation between the actual
 845 and predicted LC for scaled-down jib lengths of 30cm, 40cm, 50cm, and 60cm were 2.9, 2.6,
 846 3.19, and 1.8, respectively. The overall average deviation across all jib lengths is 2.6.
 847 Additionally, in Fig. 15, we multiplied the scale factor of a prototype with the projected LC for
 848 jib lengths of 30cm, 40cm, 50cm, and 60cm, resulting in deviations of 0.04, 0.07, 0.06, and
 849 0.07, respectively.



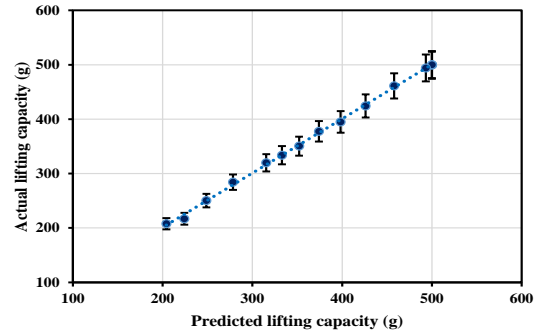
(a) Jib length 30 cm



(b) Jib length 40 cm

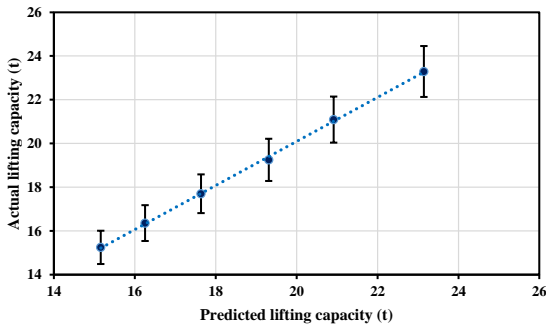


(c) Jib length 50 cm

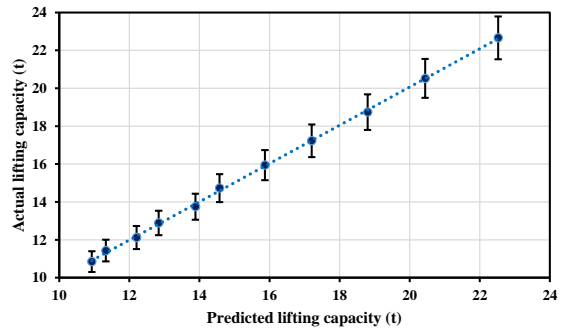


(d) Jib length 60 cm

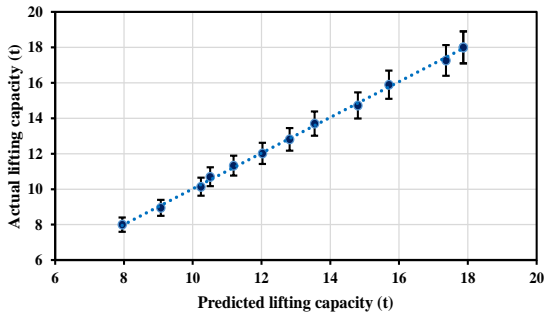
850 Fig. 14. Deviations between the actual and predicted LC for a scaled-down tower crane
 851 prototype: (1) Jib length 30cm, (b) Jib length 40cm, (c) Jib length 50cm, and (d) Jib length
 852 60cm.



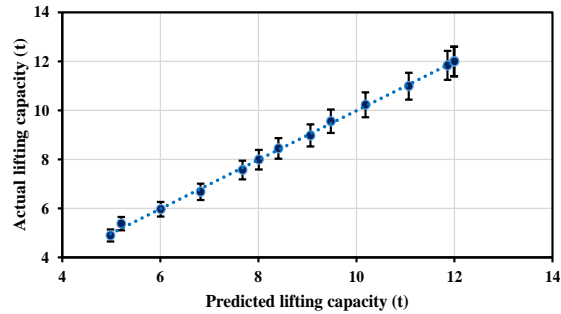
(a) Jib length 30 cm



(b) Jib length 40 cm



(c) Jib length 50 cm



(d) Jib length 60 cm

853 Fig. 15. Deviations between the actual and predicted LC for a real tower crane: (1) Jib length
 854 30cm, (b) Jib length 40cm, (c) Jib length 50cm, and (d) Jib length 60cm.

855 7. Conclusion and Future Work

856 In order to mitigate the risk of structural fatigue and aging-induced deterioration leading to
 857 failure or collapse of construction tower cranes, this study developed a digital twin-driven
 858 (DTD) framework and model for predicting the degraded lifting capacities (LC) of aging tower
 859 cranes based on real-time load and deflection data. The DTD approach enables continuous
 860 monitoring of crane safety performance and real-time prediction of degraded LC using
 861 numerical models. The DTD model successfully predicted the LC of a scaled-down prototype
 862 tower crane with a jib length of 60cm for durations of 10, 20, 30, 40, 50, 60, and 70 years,
 863 achieving MSE and R^2 values of 0.2253 and 0.9973, respectively. Using scale and similarity

864 factors, the LC for actual tower cranes with jib lengths of 30m, 40m, 50m, and 60m was
865 computed with an average deviation of 0.06%. This research contributes to understanding
866 digital twin applications in the construction industry, particularly in predictive maintenance,
867 aging infrastructure management, data-driven approaches, safety, reliability, and
868 interdisciplinarity. The findings of this study also have broader applicability beyond the
869 construction industry and can be implemented in other sectors facing similar infrastructure and
870 predictive maintenance challenges.

871 While the results of this research are promising in predicting the degraded LC of aging
872 tower cranes using the DTD approach, some areas can be further improved. Firstly, to enhance
873 the simulation quality of the DTD model, future research should consider replicating the crane's
874 foundation/baseplate, slewing unit, and climbing frame of an actual crane instead of relying on
875 a prototype. Secondly, the precision of the LC prediction can be improved by incorporating a
876 more comprehensive range of sensor types that capture various parameters. Thirdly,
877 automating the connection system between virtual and physical cranes would enhance the
878 efficiency of the DTD framework. Fourthly, it is recommended to identify the critical members
879 through FEA of the truss-type structure rather than analyzing the overall crane structure. This
880 can be achieved by considering detailed modeling and comprehensive analysis, resulting in a
881 more focused and accurate assessment of the critical components. Lastly, considering the actual
882 working conditions of the crane in numerical models can improve the accuracy of predicting
883 degradation in LC.

884 Overall, this study highlights the potential of DTD approaches in enhancing the efficiency,
885 safety, and decision-making related to aging tower cranes on construction sites. By providing
886 a continuous monitoring system for crane safety, the DTD framework can assist operators in
887 performing lifting operations with safe and degraded loads, thereby preventing unexpected
888 failures and damages while improving workplace monitoring and safety. These findings
889 present valuable opportunities for future research to advance the field further and enhance crane
890 safety in construction sites.

891 **Data availability statement**

892 This paper contains all the data generated or analyzed during this study.

893 **Declaration of competing interest**

894 The authors declare no conflict of interest.

895 **Data availability**

896 Data will be made available on request.

897 **Acknowledgment**

898 The authors would like to acknowledge "The Hong Kong Polytechnic University (PolyU)" for
899 providing and supporting the first author under "The Hong Kong Polytechnic University
900 Presidential Ph.D. Fellowship Scheme (PPFS)."

901 **References**

- 902 [1] *Code of Practice for Safe Use of Tower Cranes*,
903 http://www.labour.gov.hk/eng/public/content2_8b.htm.<http://www.labour.gov.hk/eng/tele>
904 [/osh.htm](http://www.labour.gov.hk/eng/tele/osh.htm).
- 905 [2] Gu J, Qin Y, Xia Y, et al. Failure Analysis and Prevention for Tower Crane as Sudden Unloading.
906 *Journal of Failure Analysis and Prevention* 2021; 21: 1590–1595.
- 907 [3] Shin IJ. Factors that affect safety of tower crane installation/dismantling in construction
908 industry. *Saf Sci* 2015; 72: 379–390.
- 909 [4] Guo P, Ma X, Zhang W, et al. Study of Fault Detection of Bridge Crane Wheel based on Fourier
910 Transform. In: *ACM International Conference Proceeding Series*. Association for Computing
911 Machinery, 2021, pp. 23–27.
- 912 [5] Kulka J, Mantic M, Faltinova E, et al. Failure analysis of the foundry crane to increase its
913 working parameters. *Eng Fail Anal* 2018; 88: 25–34.
- 914 [6] Vukelic G, Pastorcic D, Vizentin G. Failure analysis of a crane gear shaft. In: *Procedia Structural*
915 *Integrity*. Elsevier B.V., 2019, pp. 406–412.
- 916 [7] Das S, Mukhopadhyay G, Bhattacharyya S. Failure analysis of a 40 ton crane hook at a Hot
917 Strip Mill. In: *MATEC Web of Conferences*. EDP Sciences, 2018. Epub ahead of print 25 May
918 2018. DOI: 10.1051/mateconf/201816510006.
- 919 [8] Pal U, Mukhopadhyay G, Sharma A, et al. Failure analysis of wire rope of ladle crane in steel
920 making shop. *Int J Fatigue* 2018; 116: 149–155.
- 921 [9] Lee J, Phillips I, Lynch Z. Causes and prevention of mobile crane-related accidents in South
922 Korea. *International Journal of Occupational Safety and Ergonomics* 2020; 1–10.
- 923 [10] Steven Chun-yin HH, Hon KWOK Wai-keung J, Hon SHIU Ka-fai J, et al. *Legislative Council*.
924 2022.
- 925 [11] Lan Q, Zhang D, Li Y. *Analysis on the Current Situation and Countermeasures of Elevator*
926 *Safety in China*. 2017.
- 927 [12] Linda Levine. *Worker Safety in the Construction Industry: The Crane and Derrick Standard*.
928 2008.
- 929 [13] Fang Y, Cho YK. Effectiveness Analysis from a Cognitive Perspective for a Real-Time Safety
930 Assistance System for Mobile Crane Lifting Operations. *J Constr Eng Manag*; 143. Epub ahead
931 of print April 2017. DOI: 10.1061/(asce)co.1943-7862.0001258.
- 932 [14] Kalairassan G, Boopathi M, Mohan RM. Analysis of load monitoring system in hydraulic
933 mobile cranes. In: *IOP Conference Series: Materials Science and Engineering*. Institute of
934 Physics Publishing, 2017. Epub ahead of print 3 December 2017. DOI: 10.1088/1757-
935 899X/263/6/062045.
- 936 [15] Shaikh AA, Kumar DD. Lifting capacity enhancement of a crawler crane by improving stability.
937 *Journal of Theoretical and Applied Mechanics (Poland)* 2016; 54: 219–227.
- 938 [16] Neitzel RL, Seixas NS, Ren KK. A Review of Crane Safety in the Construction Industry. *Appl*
939 *Occup Environ Hyg* 2001; 16: 1106–1117.

- 940 [17] Rayco Wylie. *R147 WIRELESS ANTI-TWO-BLOCK INDICATOR Installation and Operation*
941 *Manual*, www.craneindicators.com (2012).
- 942 [18] Walbridge S, Nik-Bakht M, Tsun K, et al. *Lecture Notes in Civil Engineering*,
943 <https://link.springer.com/bookseries/15087> (2022).
- 944 [19] Elgendi E-BO, Shawki KM, Ashraf Mohy A. Video analysis for tower crane production rate
945 estimation. *Journal of Information Technology in Construction* 2023; 28: 138–150.
- 946 [20] Chen A, Jacob M, Shoshani G, et al. Using computer vision, image analysis and UAVs for the
947 automatic recognition and counting of common cranes (*Grus grus*). *J Environ Manage*; 328.
948 Epub ahead of print 15 February 2023. DOI: 10.1016/j.jenvman.2022.116948.
- 949 [21] Roman RC, Precup RE, Petriu EM, et al. Combination of data-driven active disturbance
950 rejection and Takagi-Sugeno fuzzy control with experimental validation on tower crane
951 systems. *Energies (Basel)*; 12. Epub ahead of print 24 April 2019. DOI: 10.3390/en12081548.
- 952 [22] Roman RC, Precup RE, Petriu EM. Hybrid data-driven fuzzy active disturbance rejection
953 control for tower crane systems. *Eur J Control* 2021; 58: 373–387.
- 954 [23] Tran VT, Thom Pham H, Yang BS, et al. Machine performance degradation assessment and
955 remaining useful life prediction using proportional hazard model and support vector machine.
956 *Mech Syst Signal Process* 2012; 32: 320–330.
- 957 [24] Liu P, Chi HL, Li X, et al. Effects of dataset characteristics on the performance of fatigue
958 detection for crane operators using hybrid deep neural networks. *Autom Constr*; 132. Epub
959 ahead of print 1 December 2021. DOI: 10.1016/j.autcon.2021.103901.
- 960 [25] Jiang W, Ding L, Zhou C. Digital twin: Stability analysis for tower crane hoisting safety with a
961 scale model. *Autom Constr*; 138. Epub ahead of print 1 June 2022. DOI:
962 10.1016/j.autcon.2022.104257.
- 963 [26] Deebak BD, Al-Turjman F. Digital-twin assisted: Fault diagnosis using deep transfer learning
964 for machining tool condition. *International Journal of Intelligent Systems*. Epub ahead of print
965 2021. DOI: 10.1002/int.22493.
- 966 [27] Wu Y, Zhou L, Zheng P, et al. A digital twin-based multidisciplinary collaborative design
967 approach for complex engineering product development. *Advanced Engineering Informatics*;
968 52. Epub ahead of print 1 April 2022. DOI: 10.1016/j.aei.2022.101635.
- 969 [28] Wu L, Leng J, Ju B. Digital twins-based smart design and control of ultra-precision machining:
970 A review. *Symmetry*; 13. Epub ahead of print 1 September 2021. DOI: 10.3390/sym13091717.
- 971 [29] Liu J, Cao X, Zhou H, et al. A digital twin-driven approach towards traceability and dynamic
972 control for processing quality. *Advanced Engineering Informatics*; 50. Epub ahead of print 1
973 October 2021. DOI: 10.1016/j.aei.2021.101395.
- 974 [30] Liu J, Cao X, Zhou H, et al. A digital twin-driven approach towards traceability and dynamic
975 control for processing quality. *Advanced Engineering Informatics*; 50. Epub ahead of print 1
976 October 2021. DOI: 10.1016/j.aei.2021.101395.
- 977 [31] Cheng DJ, Zhang J, Hu ZT, et al. A Digital Twin-Driven Approach for On-line Controlling Quality
978 of Marine Diesel Engine Critical Parts. *International Journal of Precision Engineering and*
979 *Manufacturing* 2020; 21: 1821–1841.

- 980 [32] Zhu Z, Xi X, Xu X, et al. Digital Twin-driven machining process for thin-walled part
981 manufacturing. *J Manuf Syst* 2021; 59: 453–466.
- 982 [33] Jia W, Wang W, Zhang Z. From simple digital twin to complex digital twin part II: Multi-
983 scenario applications of digital twin shop floor. *Advanced Engineering Informatics*; 56. Epub
984 ahead of print 1 April 2023. DOI: 10.1016/j.aei.2023.101915.
- 985 [34] Shen X, Li X, Zhou B, et al. Dynamic knowledge modeling and fusion method for custom
986 apparel production process based on knowledge graph. *Advanced Engineering Informatics*;
987 55. Epub ahead of print 1 January 2023. DOI: 10.1016/j.aei.2023.101880.
- 988 [35] Liu X, Jiang D, Tao B, et al. A systematic review of digital twin about physical entities, virtual
989 models, twin data, and applications. *Advanced Engineering Informatics* 2023; 55: 101876.
- 990 [36] Kušić K, Schumann R, Ivanjko E. A digital twin in transportation: Real-time synergy of traffic
991 data streams and simulation for virtualizing motorway dynamics. *Advanced Engineering
992 Informatics*; 55. Epub ahead of print 1 January 2023. DOI: 10.1016/j.aei.2022.101858.
- 993 [37] Yang X, Ran Y, Zhang G, et al. A digital twin-driven hybrid approach for the prediction of
994 performance degradation in transmission unit of CNC machine tool. *Robot Comput Integr
995 Manuf*; 73. Epub ahead of print 1 February 2022. DOI: 10.1016/j.rcim.2021.102230.
- 996 [38] Sadeghi S, Soltanmohammadlou N, Rahnamayiezekavat P. A systematic review of scholarly
997 works addressing crane safety requirements. *Saf Sci*; 133. Epub ahead of print 1 January
998 2021. DOI: 10.1016/j.ssci.2020.105002.
- 999 [39] Sulankivi K, Kiviniemi M, Mäkelä T. *BIM-based Site Layout and Safety Planning*,
1000 <https://www.researchgate.net/publication/38289116> (2014).
- 1001 [40] Shin IJ. Factors that affect safety of tower crane installation/dismantling in construction
1002 industry. *Saf Sci* 2015; 72: 379–390.
- 1003 [41] Chang YC, Hung WH, Kang SC. A fast path planning method for single and dual crane
1004 erections. In: *Automation in Construction*. 2012, pp. 468–480.
- 1005 [42] Sadeghi H, Zhang X, Mohandes SR. Developing an ensemble risk analysis framework for
1006 improving the safety of tower crane operations under coupled Fuzzy-based environment. *Saf
1007 Sci*; 158. Epub ahead of print 1 February 2023. DOI: 10.1016/j.ssci.2022.105957.
- 1008 [43] Shapira A, Asce F, Lyachin B. Identification and Analysis of Factors Affecting Safety on
1009 Construction Sites with Tower Cranes. DOI: 10.1061/ASCE0733-93642009135:124.
- 1010 [44] Vukelic G, Pastorcic D, Vizentin G, et al. Failure investigation of a crane gear damage. *Eng Fail
1011 Anal*; 115. Epub ahead of print 1 September 2020. DOI: 10.1016/j.engfailanal.2020.104613.
- 1012 [45] Guerra-Fuentes L, Torres-López M, Hernandez-Rodriguez MAL, et al. Failure analysis of steel
1013 wire rope used in overhead crane system. *Eng Fail Anal*; 118. Epub ahead of print 1
1014 December 2020. DOI: 10.1016/j.engfailanal.2020.104893.
- 1015 [46] Wu B, Tang Y, Li Z, et al. Fatigue damage accumulation modelling of critical components
1016 subjected to moving crane loads in reinforced-concrete industrial buildings. *Eng Fail Anal*;
1017 119. Epub ahead of print 1 January 2021. DOI: 10.1016/j.engfailanal.2020.104951.

- 1018 [47] Zhang X, Liu L, Wu F, et al. Digital Twin-Driven Surface Roughness Prediction Based on Multi-
1019 sensor Fusion. In: *Lecture Notes in Electrical Engineering*. Springer Science and Business
1020 Media Deutschland GmbH, 2021, pp. 230–237.
- 1021 [48] Zhuang K, Shi Z, Sun Y, et al. Digital twin-driven tool wear monitoring and predicting method
1022 for the turning process. *Symmetry (Basel)*; 13. Epub ahead of print 1 August 2021. DOI:
1023 10.3390/sym13081438.
- 1024 [49] Kong F, Lu Z, Kong L, et al. Information field in a manufacturing System: Concepts,
1025 measurements and applications. *Advanced Engineering Informatics*; 56. Epub ahead of print 1
1026 April 2023. DOI: 10.1016/j.aei.2023.101946.
- 1027 [50] Jiang Y, Li M, Wu W, et al. Multi-domain ubiquitous digital twin model for information
1028 management of complex infrastructure systems. *Advanced Engineering Informatics*; 56. Epub
1029 ahead of print 1 April 2023. DOI: 10.1016/j.aei.2023.101951.
- 1030 [51] Pauwels P, de Koning R, Hendriks B, et al. Live semantic data from building digital twins for
1031 robot navigation: Overview of data transfer methods. *Advanced Engineering Informatics*; 56.
1032 Epub ahead of print 1 April 2023. DOI: 10.1016/j.aei.2023.101959.
- 1033 [52] He F, Ong SK, Nee AYC. An integrated mobile augmented reality digital twin monitoring
1034 system. *Computers*; 10. Epub ahead of print 1 August 2021. DOI:
1035 10.3390/computers10080099.
- 1036 [53] Zhao R, Yan D, Liu Q, et al. Digital twin-driven cyber-physical system for autonomously
1037 controlling of micro punching system. *IEEE Access* 2019; 7: 9459–9469.
- 1038 [54] Christiad GK. Digital twin approach for tool wear monitoring of micro-milling. In: *Procedia*
1039 *CIRP*. Elsevier B.V., 2020, pp. 1532–1537.
- 1040 [55] Liu J, Du X, Zhou H, et al. A digital twin-based approach for dynamic clamping and positioning
1041 of the flexible tooling system. In: *Procedia CIRP*. Elsevier B.V., 2019, pp. 746–749.
- 1042 [56] *Unit II ISO/OSI Model in Communication Networks*.
- 1043 [57] Cao X, Zhao G, Xiao W. Digital Twin-oriented real-time cutting simulation for intelligent
1044 computer numerical control machining. *Proc Inst Mech Eng B J Eng Manuf* 2022; 236: 5–15.
- 1045 [58] Priyanka EB, Thangavel S. Multi-type feature extraction and classification of leakage in oil
1046 pipeline network using digital twin technology. *J Ambient Intell Humaniz Comput*. Epub ahead
1047 of print 2022. DOI: 10.1007/s12652-022-03818-9.
- 1048 [59] Mdot. *DEVELOPMENT OF STEEL BEAM END DETERIORATION GUIDELINES FINAL REPORT-*
1049 *JANUARY 2005 CENTER FOR STRUCTURAL DURABILITY MICHIGAN TECH TRANSPORTATION*
1050 *INSTITUTE*.
- 1051 [60] Bandara CS, Siriwardane SC, Dissanayake UI, et al. Developing a full range S-N curve and
1052 estimating cumulative fatigue damage of steel elements. *Comput Mater Sci* 2015; 96: 96–101.
- 1053 [61] Dong Q, He B, Qi Q, et al. Real-time prediction method of fatigue life of bridge crane structure
1054 based on digital twin. *Fatigue Fract Eng Mater Struct* 2021; 44: 2280–2306.
- 1055 [62] Jiang F, Ding Y, Song Y, et al. Digital Twin-driven framework for fatigue life prediction of steel
1056 bridges using a probabilistic multiscale model: Application to segmental orthotropic steel

1057 deck specimen. *Eng Struct*; 241. Epub ahead of print 15 August 2021. DOI:
1058 10.1016/j.engstruct.2021.112461.

1059 [63] Six K, Mihalj T, Trummer G, et al. Assessment of running gear performance in relation to
1060 rolling contact fatigue of wheels and rails based on stochastic simulations. *Proc Inst Mech Eng*
1061 *F J Rail Rapid Transit* 2020; 234: 405–416.

1062 [64] Taheri S, Vincent L, Le-Roux JC. A new model for fatigue damage accumulation of austenitic
1063 stainless steel under variable amplitude loading. In: *Procedia Engineering*. Elsevier Ltd, 2013,
1064 pp. 575–586.

1065 [65] Fatemi A, Vangt L. *Cumulative fatigue damage and life prediction theories: a survey of the*
1066 *state of the art for homogeneous materials*. 1998.

1067 [66] Teng Z, Wu H, Boller C, et al. Thermodynamic entropy as a marker of high-cycle fatigue
1068 damage accumulation: Example for normalized SAE 1045 steel. *Fatigue Fract Eng Mater*
1069 *Struct* 2020; 43: 2854–2866.

1070 [67] Chaboche JL, Lesne PM. *A NON-LINEAR CONTINUOUS FATIGUE DAMAGE MODEL*. 1988.

1071 [68] Benkabouche S, Guechichi H, Amrouche A, et al. A modified nonlinear fatigue damage
1072 accumulation model under multiaxial variable amplitude loading. *Int J Mech Sci* 2015; 100:
1073 180–194.

1074 [69] Cantrell JH. Dependence of microelastic-plastic nonlinearity of martensitic stainless steel on
1075 fatigue damage accumulation. *J Appl Phys*; 100. Epub ahead of print 2006. DOI:
1076 10.1063/1.2345614.

1077 [70] Pompetzki MA, Topper TH, Duquesnay DL. *The effect of compressive underloads and tensile*
1078 *overloads on fatigue damage accumulation in SAE 1045 steel*. 1990.

1079 [71] Pape JA, Neu RW. *Fretting fatigue damage accumulation in PH13-8Mo stainless steel*,
1080 www.elsevier.com/locate/ijfatigue (2001).

1081 [72] Wiethorn JD, Matthew PE, Gardiner R, et al. *TOWER CRANE LIFE EXPECTANCY AN*
1082 *EXAMINATION OF RECENT TRENDS TO ESTABLISH AGE LIMITS*.

1083 [73] Roysson S, Gustafsson J, Lindell R, et al. *EVALUATING THE LIFTING CAPACITY IN A MOBILE*
1084 *CRANE SIMULATION*.

1085 [74] Przybyłek G, Więckowski J. Method of assessing the technical condition and failure of
1086 overhead cranes designed to work in difficult conditions. *Case Studies in Construction*
1087 *Materials*; 16. Epub ahead of print 1 June 2022. DOI: 10.1016/j.cscm.2021.e00811.

1088 [75] Lee WJ, Wu H, Yun H, et al. Predictive maintenance of machine tool systems using artificial
1089 intelligence techniques applied to machine condition data. In: *Procedia CIRP*. Elsevier B.V.,
1090 2019, pp. 506–511.

1091 [76] Dong Q, He B, Qi Q, et al. Real-time prediction method of fatigue life of bridge crane structure
1092 based on digital twin. *Fatigue Fract Eng Mater Struct* 2021; 44: 2280–2306.

1093 [77] Sepasgozar SME. Differentiating digital twin from digital shadow: Elucidating a paradigm shift
1094 to expedite a smart, sustainable built environment. *Buildings*; 11. Epub ahead of print 1 April
1095 2021. DOI: 10.3390/buildings11040151.

